

Effect of single metal loading on $\text{CaO}/\text{Al}_2\text{O}_3$ pellet catalyst for biodiesel production



A Thesis Submitted in Partial Fulfillment of the Requirements
for the Degree of Master of Engineering in Chemical Engineering

Department of Chemical Engineering

FACULTY OF ENGINEERING

Chulalongkorn University

Academic Year 2020

Copyright of Chulalongkorn University

ผลของการเติมโลหะเดี่ยวบนตัวเร่งปฏิกิริยาอะดเม็ต $\text{CaO}/\text{Al}_2\text{O}_3$ สำหรับการผลิตไบโอดีเซล



วิทยานิพนธ์นี้เป็นส่วนหนึ่งของการศึกษาตามหลักสูตรปริญญาวิทยาศาสตรมหาบัณฑิต

สาขาวิชาวิศวกรรมเคมี ภาควิชาวิศวกรรมเคมี

คณะวิศวกรรมศาสตร์ จุฬาลงกรณ์มหาวิทยาลัย

ปีการศึกษา 2563

ลิขสิทธิ์ของจุฬาลงกรณ์มหาวิทยาลัย

ณัฐวดี มั่นบุปผชาติ : ผลของการเติมโลหะเดี่ยวบนตัวเร่งปฏิกิริยา

อัดเม็ด $\text{CaO}/\text{Al}_2\text{O}_3$ สำหรับการผลิตไบโอดีเซล. (Effect of single

metal loading on $\text{CaO}/\text{Al}_2\text{O}_3$ pellet catalyst for biodiesel production) อ.ที่

ปรึกษาหลัก : ศ. ดร.สุทธิชัย อัสนะบำรุงรัตน์, อ.ที่ปรึกษาร่วม : รศ. ดร.กนกวรรณ จ้าว
สุวรรณ

ไบโอดีเซลเป็นเชื้อเพลิงชีวภาพที่ยั่งยืนซึ่งส่วนใหญ่ผลิตได้จากปฏิกิริยาทรานส์เอสเทอร์ฟิเคชันโดยใช้น้ำมันพืชหรือไขมันสัตว์ ในปฏิกิริยาทรานส์เอสเทอร์ฟิเคชันที่ใช้ตัวเร่งปฏิกิริยาวิวิธพันธุ์ได้รับความนิยมสนใจอย่างมากในช่วงไม่กี่ปีที่ผ่านมา แต่เนื่องจากตัวเร่งปฏิกิริยาวิวิธพันธุ์ที่เป็นผงพบว่ามีคามดันตกคร่อมสูง (pressure drop) จึงไม่เหมาะสำหรับกระบวนการต่อเนื่อง (continuous process) โดยตัวเร่งปฏิกิริยาขึ้นรูปมีความสะดวกในการใช้งาน แต่อย่างไรก็ตามการที่มีพื้นผิวต่อปริมาตรต่ำจึงทำให้ความสามารถของตัวเร่งปฏิกิริยาในปฏิกิริยาทรานส์เอสเทอร์ฟิเคชันมีค่าลดลง งานวิจัยนี้จึงมีวัตถุประสงค์เพื่อศึกษาผลของการใส่โลหะออกไซด์บนตัวเร่งปฏิกิริยาอัดเม็ด $\text{CaO}/\text{Al}_2\text{O}_3$ เพื่อปรับปรุงความสามารถของตัวเร่งปฏิกิริยาในปฏิกิริยาทรานส์เอสเทอร์ฟิเคชัน โดยใช้ตัวเร่งปฏิกิริยาที่ได้จากการเติม 20 wt.% ของโลหะออกไซด์บนตัวเร่งปฏิกิริยาอัดเม็ด $\text{CaO}/\text{Al}_2\text{O}_3$ ขึ้นรูป ประกอบด้วย $\text{Li-CaO}/\text{Al}_2\text{O}_3$, $\text{K-CaO}/\text{Al}_2\text{O}_3$, $\text{Sr-CaO}/\text{Al}_2\text{O}_3$ และ $\text{Fe-CaO}/\text{Al}_2\text{O}_3$ ซึ่งสังเคราะห์ด้วยวิธีการทำให้เอิบชุ่มพอดี (incipient wetness impregnation) พบว่าตัวเร่งปฏิกิริยาอัดเม็ด $\text{K-CaO}/\text{Al}_2\text{O}_3$ ได้ผลผลิตไบโอดีเซลสูงสุด (95.5%) ภายใต้อัตราส่วน 12:1 โมลเมทานอลต่อน้ำมันที่ 65 °C ปริมาณตัวเร่งปฏิกิริยา 10 wt.% เป็นเวลา 6 ชั่วโมง ค่าความเป็นเบสของตัวเร่งปฏิกิริยานี้มีค่าเท่ากับ 2.40 mmol/g และจากการศึกษาค่า TOF ช่วงเริ่มต้นพบว่ามีความสัมพันธ์ระหว่างความเป็นเบสกับความสามารถของตัวเร่งปฏิกิริยา นอกจากนี้ความแข็งแรงเชิงกล (mechanical strength) ของตัวเร่งปฏิกิริยาอัดเม็ด $\text{K-CaO}/\text{Al}_2\text{O}_3$ เพิ่มขึ้นเมื่อเทียบกับตัวเร่งปฏิกิริยาอัดเม็ด $\text{CaO}/\text{Al}_2\text{O}_3$ แต่อย่างไรก็ตามยังพบปัญหาการชะล้าง (leaching) ของตัวเร่งปฏิกิริยาอัดเม็ด $\text{K-CaO}/\text{Al}_2\text{O}_3$ เกิดขึ้นระหว่างปฏิกิริยาทรานส์เอสเทอร์ฟิเคชัน

สาขาวิชา วิศวกรรมเคมี

ปีการศึกษา 2563

ลายมือชื่อนิสิต

ลายมือชื่อ อ.ที่ปรึกษาหลัก

ลายมือชื่อ อ.ที่ปรึกษาร่วม

6270091021 : MAJOR CHEMICAL ENGINEERING

KEYWORD: Transesterification, Pellet catalyst, Biodiesel

Nattawadee Munbupphachart : Effect of single metal loading on CaO/Al₂O₃ pellet catalyst for biodiesel production .

Advisor: Prof. SUTTICHAJ ASSABUMRUNGRAT, Ph.D. Co-advisor: Assoc. Prof. Kanokwan Ngaosuwan, D.Eng.

Biodiesel is a sustainable biofuel mainly derived from transesterification of vegetable oil or animal fat. Transesterification is increasingly being catalyzed by heterogeneous catalysts in recent years. As a result of a high-pressure drop, solid base catalysts in a powder form are not suitable for a continuous process. A pellet catalyst is more convenient, but it has lower surface per volume as well as lower in its catalytic activity for transesterification. This research aims at studying the effect of metal oxides loading on CaO/Al₂O₃ pellet catalyst for improvement of catalytic activity of transesterification. The 20 wt.% single metal loading of metal oxides on CaO/Al₂O₃ pellet catalysts including Li-CaO/Al₂O₃, K-CaO/Al₂O₃, Sr-CaO/Al₂O₃, and Fe-CaO/Al₂O₃ were synthesized by incipient impregnation method. The K-CaO/Al₂O₃ pellet catalyst gave the highest biodiesel yield (95.5%) under 12:1 methanol to oil molar ratio, 65 °C, 10 wt.% catalysts and 6 h reaction time. Its total basicity was found to be 2.40 mmol/g. The initial TOF was determined and found the relationship between the basicity and its catalytic activity. In addition, the mechanical strength of K-CaO/Al₂O₃ pellet catalyst was increased when compared with the bare CaO/Al₂O₃ pellet catalyst. Unfortunately, the leaching problem of K-CaO/Al₂O₃ pellet catalyst was observed during the transesterification.

Field of Study: Chemical Engineering

Student's Signature

Academic Year: 2020

Advisor's Signature

Co-advisor's Signature

ACKNOWLEDGEMENTS

First and foremost, I would like to express gratitude to Professor Suttichai Assabumrungrat and Associate Professor Kanokwan Ngaosuwan, my advisor and co-advisor, for their unwavering support of my research and studies, as well as their motivation, enthusiasm, vast knowledge, and grateful assistance has encouraged for my research and inspire my life. Their advice was essential during the research and writing of this thesis. For my thesis, it would not have been possible without their great direction. In addition, my performing under their direction has been a great experience for me.

Besides my adviser, I would like to sincere thanks the chairman Professor Paisan Kittisupakorn, and the rest of committees: Professor Joongjai Panpranot, and Associate Professor Atthapon Srifa for their guidance, insightful suggestions, and great feedback.

My sincerest appreciation also goes to the technicians and members of the Center of Excellence on Catalysis and Catalytic Reaction Engineering (CECC) laboratory for their assistance.

A particular thanks, I would like to thank my parents for financial assistance and supporting me spiritually throughout my life, particularly their always understand, care, and persist, making the difficult task of writing the dissertation worthy. I would like to express my gratitude to my friends for their continuing support, encouragement, and inspection. Finally, to my best friend, who is always a source of delight for me and who stands by me in hard moments.

Nattawadee Munbupphachart

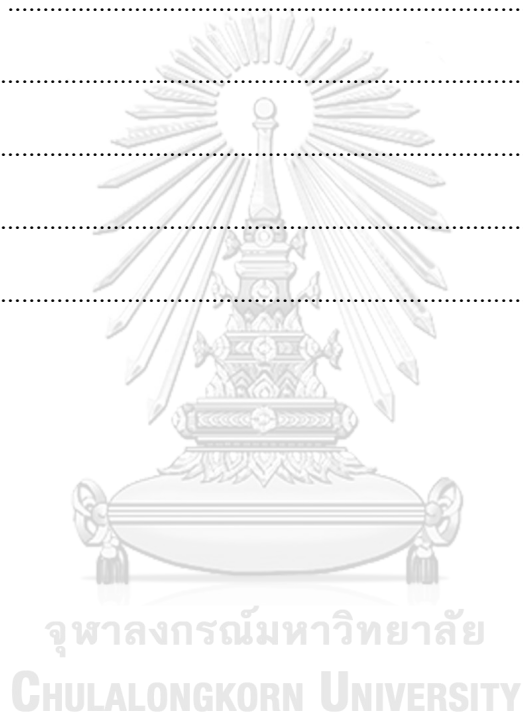
TABLE OF CONTENTS

| | Page |
|--|------|
| | iii |
| ABSTRACT (THAI)..... | iii |
| | iv |
| ABSTRACT (ENGLISH)..... | iv |
| ACKNOWLEDGEMENTS..... | v |
| TABLE OF CONTENTS..... | vi |
| LIST OF FIGURES..... | 1 |
| LIST OF FIGURES (CONT.)..... | 2 |
| LIST OF TABLES..... | 3 |
| CHAPTER 1..... | 4 |
| 1.1 Introduction..... | 4 |
| 1.2 Objectives..... | 5 |
| 1.3 Scope of research..... | 5 |
| 1.4 Research methodology..... | 7 |
| CHAPTER 2..... | 8 |
| 2.1 Transesterification..... | 8 |
| 2.2 Biodiesel..... | 9 |
| 2.3 Catalyst for biodiesel production..... | 12 |
| 2.4 Base catalyst for biodiesel production..... | 13 |
| 2.5 Calcium oxide (CaO)..... | 13 |
| 2.6 Metal loading catalyst for biodiesel production..... | 15 |

| | |
|---|----|
| 2.7 Extruded catalyst..... | 15 |
| 2.8 Mass transfer for heterogeneous catalyst..... | 16 |
| 2.9 Literature reviews..... | 17 |
| 2.7.1 Catalyst forming | 17 |
| 2.7.2 Metal loading on catalyst | 19 |
| 3.1 Chemicals..... | 21 |
| 3.2 Procedure for catalyst preparation..... | 22 |
| 3.3 Catalytic activity test | 22 |
| 3.5 Catalyst characterization..... | 22 |
| 3.5.1 Thermogravimetric analysis/differential scanning calorimeter (TGA/DSC) | 22 |
| 3.5.2 X-ray diffraction (XRD)..... | 23 |
| 3.5.3 Scanning electron microscope and energy dispersive X-ray spectrometer (SEM/EDX)..... | 23 |
| 3.5.4 Fourier-transform infrared spectroscopy (FTIR) | 23 |
| 3.5.5 Hammett indicators..... | 23 |
| 3.5.6 CO ₂ temperature programmed desorption of carbon dioxide (CO ₂ -TPD). | 24 |
| 3.5.7 N ₂ adsorption–desorption isotherms by using Brunauer-Emmett-Teller method (BET)..... | 24 |
| 3.5.8 Mechanical strength | 24 |
| 3.5.9 Biodiesel (FAME) production analysis using gas chromatography according to EN 14103 standard..... | 24 |
| 3.5.10 The initial turnover frequency (TOF, time ⁻¹) was calculation by using the initial rate and total basicity as followed by Eq. (3.2) [56]. | 26 |
| CHAPTER 4..... | 27 |
| 4.1 Catalyst characterization of metal doped on CaO/Al ₂ O ₃ pellet catalysts..... | 27 |

| | |
|--|----|
| 4.1.1 Thermogravimetric analysis/differential scanning calorimeter (TGA/DSC) | 27 |
| 4.1.2 X-ray diffraction (XRD)..... | 28 |
| 4.1.3 Fourier-transform infrared spectroscopy (FTIR) | 31 |
| 4.1.4 Surface morphology of CaO/Al ₂ O ₃ pellet catalyst with metal doped using scanning electron microscope and energy dispersive X-ray spectrometer (SEM/EDX)..... | 32 |
| 4.1.5 N ₂ adsorption–desorption results by using Brunauer-Emmett-Teller method (BET)..... | 36 |
| 4.1.6 CO ₂ temperature programmed desorption of carbon dioxide (CO ₂ -TPD). | 39 |
| 4.1.7 Hammett indicators..... | 41 |
| 4.1.8 Mechanical strength..... | 42 |
| 4.2 Catalytic activity of CaO/Al ₂ O ₃ pellet catalysts via transesterification of palm oil | 43 |
| 4.2.1 Effect of size of CaO/Al ₂ O ₃ pellet catalysts on the catalytic activity of transesterification | 43 |
| 4.2.2 Effect of CaO/Al ₂ O ₃ pellet catalysts with different metal oxide on the catalytic activity of transesterification..... | 45 |
| 4.2.3 Effect of CaO/Al ₂ O ₃ pellet catalysts with different metal oxides on the initial rate and initial TOF for catalytic activity of transesterification | 46 |
| 4.2.4 Effect of leaching problem of CaO/Al ₂ O ₃ pellet catalysts with different metal oxide on the catalytic activity of transesterification | 48 |
| 4.2.4 Comparison of catalytic activity in transesterification between other literature and in this study | 50 |
| CHAPTER 5..... | 53 |
| 5.1 Conclusions | 53 |
| 5.2 Recommendation..... | 54 |

| | |
|-------------------------|----|
| APPENDIX..... | 55 |
| APPENDIX A..... | 56 |
| CALCULATIONS..... | 56 |
| APPENDIX B..... | 62 |
| HAMMETT INDICATORS..... | 62 |
| APPENDIX C..... | 64 |
| BIODIESEL YIELD..... | 64 |
| APPENDIX D..... | 65 |
| THE INITIAL TOF..... | 65 |
| REFERENCES..... | 67 |
| VITA..... | 77 |



LIST OF FIGURES

| | Page |
|--|------|
| Figure 2.1 Overall transesterification | 8 |
| Figure 2.2 Three steps of reversible transesterification | 9 |
| Figure 2.3 Fatty acid composition in various feedstocks to produce biodiesel..... | 10 |
| Figure 2.4 Individual steps of a simple, heterogeneous catalytic fluid–solid reaction | 17 |
| Figure 4.1 Thermogravimetric analysis/differential scanning calorimeter (TGA/DSC) of different metal doped on CaO/Al ₂ O ₃ pellet catalysts..... | 27 |
| Figure 4.2 X-rays diffraction of different metal doped on CaO/Al ₂ O ₃ pellet catalysts | 29 |
| Figure 4.3 Fourier transform infrared spectroscopy (FTIR) of metal doped on CaO/Al ₂ O ₃ pellet catalysts using different metal species (a) CaO/Al ₂ O ₃ , (b) Li-CaO/Al ₂ O ₃ , (c) K-CaO/Al ₂ O ₃ , (d) Sr-CaO/Al ₂ O ₃ and (e) Fe-CaO/Al ₂ O ₃ | 32 |
| Figure 4.4 The element composition of metal doped on CaO/Al ₂ O ₃ pellet catalysts using different metal species (a) CaO/Al ₂ O ₃ , (b) K-CaO/Al ₂ O ₃ , (c) Sr-CaO/Al ₂ O ₃ and (d) Fe-CaO/Al ₂ O ₃ | 35 |
| Figure 4.5 Adsorption-desorption isotherm of (a) CaO/Al ₂ O ₃ , (b) CaO/Al ₂ O ₃ +pore, (c) Li-CaO/Al ₂ O ₃ , (d) K-CaO/Al ₂ O ₃ , (e) Sr-CaO/Al ₂ O ₃ and (f) Fe-CaO/Al ₂ O ₃ pellet catalyst..... | 36 |
| Figure 4.6 Pore size distribution curves of mesoporous (a) CaO/Al ₂ O ₃ , (b) CaO/Al ₂ O ₃ +pore, (c) Li-CaO/Al ₂ O ₃ , (d) K-CaO/Al ₂ O ₃ , (e) Sr-CaO/Al ₂ O ₃ and (f) Fe-CaO/Al ₂ O ₃ pellet catalyst..... | 37 |
| Figure 4.7 CO ₂ temperature programmed desorption of carbon dioxide (CO ₂ -TPD)... | 39 |
| Figure 4.8 Effect of size of CaO/Al ₂ O ₃ pellet catalysts on the catalytic activity of transesterification..... | 44 |
| Figure 4.9 Effect of CaO/Al ₂ O ₃ pellet catalysts with different metal oxide on the catalytic activity of transesterification | 46 |
| Figure 4.10 Biodiesel yield after 1 h reaction time with different metal oxide loading on the CaO/Al ₂ O ₃ pellet catalysts. | 48 |

LIST OF FIGURES (CONT.)

Page

Figure 4.11 Effect of leaching problem on CaO/Al₂O₃ pellet catalysts with different metal oxide on the catalytic activity of transesterification.....50



LIST OF TABLES

| | Page |
|---|------|
| Table 2.1 ASTM standard for biodiesel specification..... | 10 |
| Table 2.2 EN14214 standard for biodiesel specification..... | 11 |
| Table 2.3 Temperature of formation of CaO using various precursors and calcination conditions..... | 14 |
| Table 3.1 Specification of chemical in research | 21 |
| Table 3.2 Conditions of gas chromatography analysis to determine free fatty acid methyl ester (FAME)..... | 25 |
| Table 4.1 Crystallite sizes of the each metal oxide species using different metal loading on CaO/Al ₂ O ₃ pellet catalysts | 31 |
| Table 4.2 Surface morphology of CaO/Al ₂ O ₃ pellet catalysts with metal doped by using scanning electron microscope and energy dispersive X-ray spectrometer (SEM/EDX)..... | 34 |
| Table 4.3 BET surface area of the CaO/Al ₂ O ₃ pellet catalysts with metals doping..... | 38 |
| Table 4.4 Number of basic sites of metal loading on CaO/Al ₂ O ₃ catalyst measured by CO ₂ -TPD..... | 41 |
| Table 4.5 Basic strength and basicity of metal loading on CaO/Al ₂ O ₃ catalyst measured by Hammett indication method..... | 42 |
| Table 4.6 Mechanical strength of the bare CaO/Al ₂ O ₃ and metal loading on CaO/Al ₂ O ₃ catalyst..... | 43 |
| Table 4.7 Initial TOF on CaO/Al ₂ O ₃ pellet catalysts with different metal oxide on the catalytic activity of transesterification..... | 48 |
| Table 4.8 Summarization of base catalyst for transesterification..... | 51 |

CHAPTER 1

INTRODUCTION

1.1 Introduction

The world is facing with petroleum sources depletion and global warming problems. The use of conventional fossil fuels does not only increase the emission of combustion-generated pollutants, but their costs are also increasing every year which are their drawback [2]. Recently, renewable biofuels have attracted much attention because of the increasing demand for energy resources, as well as elevated concerns about greenhouse gas emissions [3]. Biodiesel is a biofuel which is nontoxic for the engine, biodegradable and environmentally friendly with higher combustion efficiency, better lubrication and higher flash point compared to conventional diesel [4]. Biodiesel is produced from various edible and non-edible oils via transesterification. Transesterification is most interesting for bio-renewable resources, economically viable and offers a simple process for the industrial scale [5]. However, development and optimization of the reaction conditions, as well as the selection of the most active and selective catalyst, are still continuing researches for high-efficiency biodiesel production [6]. Biodiesel is successfully produced using both homogeneous and heterogeneous catalysts. A homogeneous catalyst is a conventional method to produce biodiesel due to its advantage of providing high catalytic activity under mild conditions [7]. Unfortunately, the process involving homogeneous catalysts has some limitations such as a large water requirement for catalyst separation, resulting in a higher production cost and producing more wastewater.

Recently, heterogeneous catalysts have gained more importance to catalyze transesterification, especially base heterogeneous catalysts such as CaO, MgO and hydrotalcite. The CaO catalyst in powder form has been widely used to catalyze transesterification [8]. However using a small and fine particle size catalyst in a continuous process would suffer from large pressure drop [9]. In biodiesel production, improvement in this regard can be using pellet catalyst [10]. The utilization of pellet catalyst is preferable for use in continuous process and practical

alternative to powder catalyst. A pellet catalyst could be a practical choice, but its catalytic activity can decrease due to its lower surface area per unit volume. Various factors affect the design of catalysts. Basicity of the biodiesel catalyst is one factor affecting the catalyst activity in transesterification. In general, a catalyst with high basicity can produce a higher biodiesel yield because reaction rate is faster compared to acid catalyst [11]. Various base metals have been doped on catalyst to enhance their catalytic performance [12]. Strontium oxide (SrO) is one of metal loading on the catalyst showing high catalytic activity for transesterification as compared to CaO and MgO catalysts [13]. However, the metal loading on CaO/Al₂O₃ catalyst would possibly cause leaching problem on transesterification process. The leaching of active metal can reduce catalytic activity and reusability of solid catalyst and result in the product contamination [14]. Therefore, mixed alkali earth metal oxides catalysts providing higher catalytic efficiency and stronger reusability can be obtained as compared with using pure metal oxides [15].

This work aims to enhance the catalytic performance and biodiesel yield of single metal loading on CaO/Al₂O₃ pellet catalyst using the various single metal loading (M/CaO/Al₂O₃) via transesterification of palm oil at the mild reaction condition in a 3-necks round bottom flask. Moreover, the leaching test of the single metal loading on the CaO/Al₂O₃ pellet catalyst will be investigated to gain more insight of using the pellet catalyst for biodiesel production.

1.2 Objectives

1.2.1 To study effect of different single metal metals loading on CaO/Al₂O₃ pellet catalyst for improvement of catalytic activity of transesterification

1.2.2 To study the leaching test of different single metal loading on CaO/Al₂O₃ pellet catalyst

1.3 Scope of research

1.3.1 Catalyst preparation

Single loading metals including of Sr, Li, Fe and K were loaded on CaO/Al₂O₃ pellet catalyst by incipient wetness impregnation method.

1.3.2 Characterization

The prepared metals loading on CaO/Al₂O₃ pellet catalysts were characterized using the following techniques:

1.3.2.1 Thermogravimetric analysis/differential scanning calorimeter (TGA/DSC)

1.3.2.2 X-ray diffraction (XRD)

1.3.2.3 Scanning electron microscopy (SEM)

1.3.2.4 Energy-dispersive X-ray spectroscopy (EDX)

1.3.2.5 Fourier-transform infrared spectroscopy (FT-IR)

1.3.2.6 Hammett indicators method

1.3.2.7 CO₂ temperature programmed desorption (CO₂-TPD)

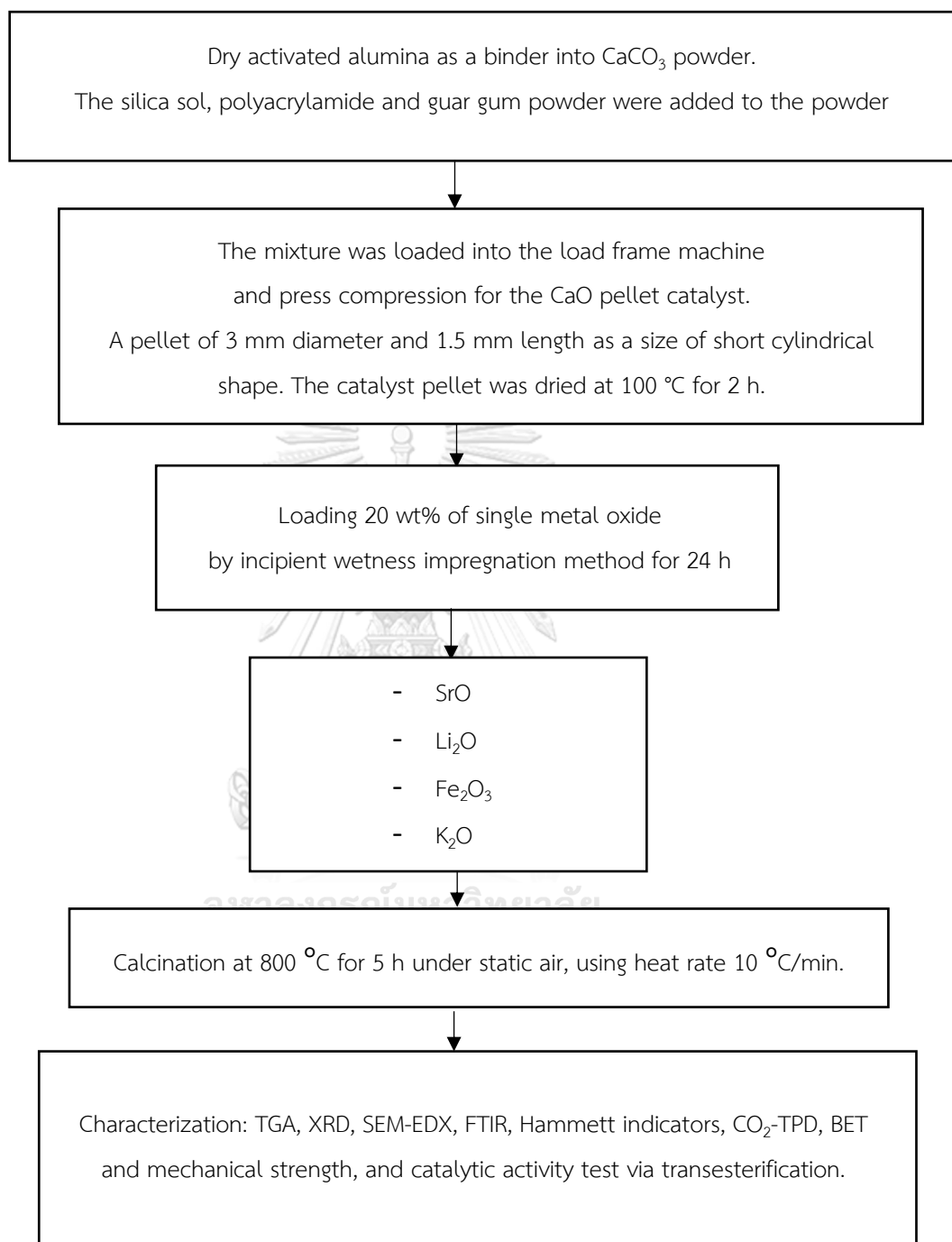
1.3.2.8 N₂ adsorption-desorption isotherms by using Brunauer-Emmett-Teller method (BET)

1.3.2.9 Mechanical strength

1.3.3 Catalytic performance of transesterification of palm oil and methanol was determined using the single metals loading on CaO/Al₂O₃ pellet catalysts using methanol to oil molar ratio of 12:1, reaction temperature of 65 °C, 10 wt.% of catalyst, 600 rpm and 6 h reaction time.

1.3.4 Leaching test of the single metal loading on CaO/Al₂O₃ pellet catalysts was further investigated via transesterification.

1.4 Research methodology



CHAPTER 2

BACKGROUND AND LITERATURE REVIEW

2.1 Transesterification

The reaction between oils (triglycerides) and short chain alcohol (mainly using methanol or ethanol) with a strong base or strong acid catalyst to produce biodiesel and glycerol as a byproduct. In transesterification, the feedstocks can be a vegetable oils or animal fats or used cooking oils (UCO) [1] and usually react with methanol (CH₃OH) as an alcohol as illustrated in Figure 2.1. According to overall reaction, the stoichiometry of triglycerides and methanol is 1 to 3. Using excessive of methanol can provide the reaction forward to produce more biodiesel.

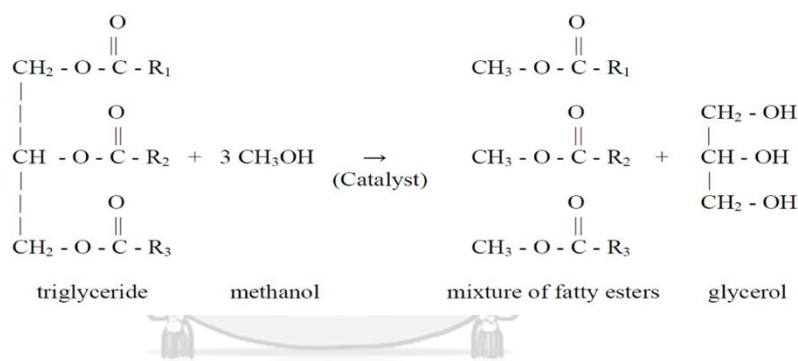


Figure 2.1 Overall transesterification [1]

CHULALONGKORN UNIVERSITY

Transesterification is a reversible reaction composed of three consecutive steps. In the first step starts from triglycerides to diglycerides, the second step of diglycerides is converted to monoglycerides and monoglycerides in the final step is converted to glycerol and biodiesel (R'COOR₁, R'COOR₂ and R'COOR₃) is produced with all three steps as shown in Figure 2.2 [16]. The product and byproduct are mechanically separated by density of any composition, glycerol has a higher density than that of fatty acid methyl ester (FAME, biodiesel) as can be seen in the bottom of vessel. Crude glycerol can be purified to increase valuable which is used as a raw material of cosmetic and food, as well as oleochemical industry.

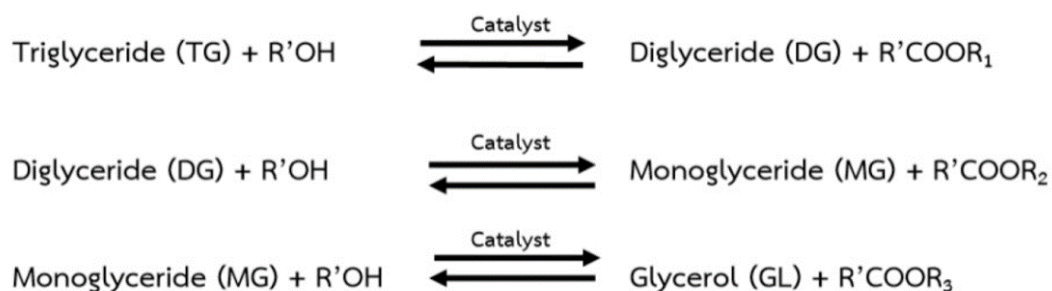


Figure 2.2 Three steps of reversible transesterification [16]

2.2 Biodiesel

A liquid fuel can be effectively substitute for diesel fuel, biodiesel is a renewable energy and nontoxic to diesel engines. Biodiesel is mainly produced via transesterification. The quality of biodiesel is depended on production process and type of oils, since different oil contains different of fatty acids. In generally, the various of fatty acids have found in biodiesel more than 10 types (C12-C22) and 90% of carbon chains consist of C16 - C18 which may be a saturated or unsaturated fatty acid [17] as shown in Figure 2.3. Hence, biodiesel grade should be accepted from industry specification grade to ensure suitable that performance. In Thailand, the characteristic and quality of biodiesel is followed from the EN14214 standard [18] while ASTM D 6751 standard is used in the United States [19]. Two categorized methods for biodiesel specification consist of chemical and physical method such as flash point, viscosity, etc. The important chemical and physical properties of biodiesel following on ASTM and EN14214 are showed in Table 2.1 and 2.2., respectively.

Biodiesel is commonly as pure biodiesel, the B100 is fuel that contains only biodiesel, but if biodiesel is mixed with diesel fuel will use the BXX which means containing XX% of biodiesel and the XX subtract from 100% is diesel. For example, B20 means oil 20% biodiesel blended with 80% diesel [20]. Today, diesel vehicles used that 80% diesel (B20) more than 78% of diesel fuel [21].

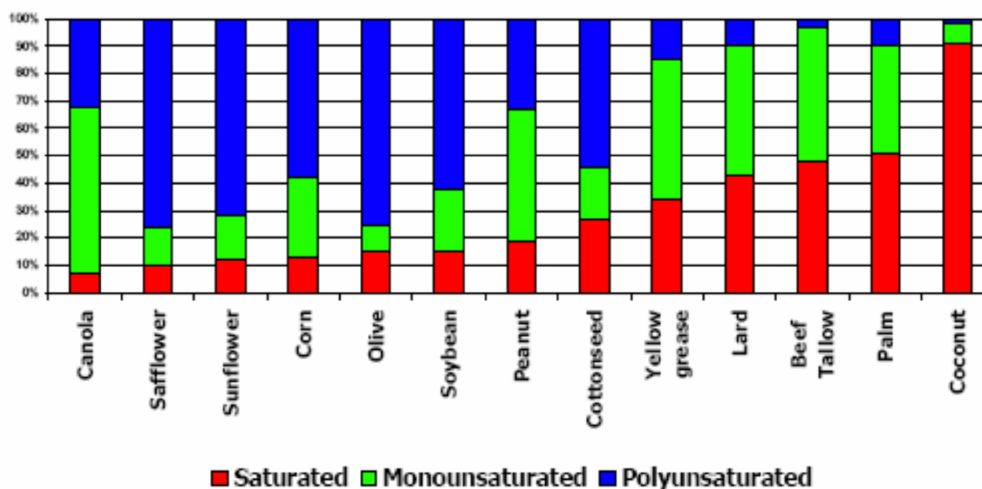


Figure 2.3 Fatty acid composition in various feedstocks to produce biodiesel [17]

Table 2.1 ASTM standard for pure biodiesel (100%) [19]

| Property | ASTM method | Limits | Units |
|---------------------------------|-------------------|-------------|--------------------|
| Flash point | 93 | 100.0 min | °C |
| Water | 1796 | 0.050 max | vol% |
| Carbon residue, 100 % sample | 4530 ^b | 0.050 max | wt% |
| Sulfated ash | 874 | 0.020 max | wt% |
| Kinematic viscosity, 40°C | 445 | 1.9–6.0 | mm ² /s |
| Sulfur | 2622 | 0.050 max | wt% |
| Cetane | 613 | 40 min | |
| Cloud point | 2500 | By customer | °C |
| Copper strip corrosion | 130 | No. 3b max | |
| Acid number | 644 | 0.80 max | mg KOH/g |
| Free glycerol | GC ^c | 0.20 max | wt% |
| Total glycerol | GC ^c | 0.40 max | wt% |

^aThis specification is the process of being evaluated by ASTM.

^bor equivalent ASTM testing method.

^cAustrian (Christina Plank) update of USDA test method.

Table 2.2 EN14214 standard for biodiesel specification [22].

| Properties | Units | EU EN14214 (2003) |
|-------------------------|------------------------|----------------------|
| Ester content | wt% | 96.5 min |
| Density | kg/m ³ | 860-900 |
| Viscosity | mm ² /s | 3.5-5.0 |
| Flashpoint | °C | 120 min |
| Sulfur content | wt% | 0.0010 max |
| Carbon residual (100 %) | wt% | -- |
| Cetane number | -- | 51.0 min |
| Sulfated ash | wt% | 0.02 max |
| Water content | mg/kg | 500 max |
| Water and sediment | vol% | -- |
| Total contamination | mg/kg | 24 max |
| Copper corrosion | rating | Class 1 |
| Oxidation stability | h | 6.0 min |
| Acid value | mgKOH/g | 0.50 max |
| Iodine value | g I ₂ /100g | 120 max |
| Methyl linolenate | wt% | 12.0 max |
| Polyunsaturated FAME | wt% | 1 max |
| Methanol content | wt% | 0.20 max |
| Monoglyceride content | wt% | 0.80 max |
| Diglyceride content | wt% | 0.20 max |
| Triglyceride content | wt% | 0.20 max |
| Free glycerol content | wt% | 0.02 max |
| Total glycerol content | wt% | 0.25 max |

| Properties | Units | EU EN14214 (2003) |
|-----------------------------|-------|----------------------|
| Group I metals (Na and K) | mg/kg | 5.0 max |
| Group II metals (Ca and Mg) | mg/kg | 5.0 max |
| Phosphorus content | mg/kg | 10.0 max |

2.3 Catalyst for biodiesel production

Biodiesel is mainly produced by transesterification. This reaction can be catalyzed by acid, base and enzyme catalysts. The catalyst can be either in a homogeneous or heterogeneous reaction. Homogeneous catalyst is generally used in the conventional transesterification since the reaction is faster and requires the lower catalyst loading compared to heterogeneous catalyst [23]. Nevertheless, homogeneous catalyst is difficult to separate and requires more equipment, resulting in higher production cost [24]. Hence, heterogeneous catalyst is recently used in transesterification and get more attention especially in the research field because solid catalyst can be reused in several times and simple the product purification [25]. From above mentioned, there are 3 types of catalyst used for biodiesel production as acid, base and enzyme catalysts [26]. Mainly, homogeneous base catalysts are mostly used in transesterification process because of carried out a shorter period reaction time than that of acid catalyst and proper conditions [7] while, homogeneous acid catalysts are suitable when the feedstock has high amount of FFA (free fatty acid) since their capability can be successful attack with FFA via esterification to produce biodiesel [11]. However, both homogeneous acid and base catalysts still have problems with separation and purification process. The enzymatic transesterification can eliminate undesired by-products, soaps, di- and monoglyceride which impede in the glycerol separation [27]. These advantages of enzyme catalyst that proceed in mild condition and apply to wide range of FFA (0.5-80%) [28]. Nonetheless, it has a high cost of enzyme, slow reaction rate and enzyme deactivation.

Therefore, heterogeneous catalysts have received attention to develop for biodiesel production [29]. Heterogeneous acid catalyst mostly comprises of sulfated metal oxide and sulfonic but, the main problem for using acid catalyst is related to the corrosive problem and required a large of alcohol to oil molar ratio and high catalyst concentration. Among, heterogeneous base catalyst gives the remarkable catalytic activity for biodiesel production, this type of catalyst has been investigated to develop structure and ability for high efficiency biodiesel production.

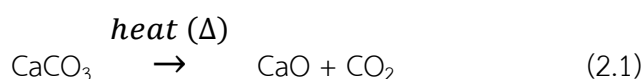
2.4 Base catalyst for biodiesel production

From industrial biodiesel production process, base catalysts are usually used in this process. NaOH and KOH are widely used to catalyze transesterification due to their low price and high catalytic activities [30]. In general, the efficiency of either homogeneous or heterogeneous base catalyzed is higher than the acid catalyzed transesterification because the different in the mechanistic pathway leads to obtain the mild reaction condition compared to acid catalyst [31]. It should be noted that one major drawback of homogeneous catalyst is separation process. Thus, heterogeneous base catalyst poses more potential for biodiesel production. Many researches are interesting in the using base catalyst, especially alkaline earth oxide to catalyze transesterification. The catalytic activity of famous base solid catalyst: BaO>SrO>CaO>MgO which is the similar order of their basicity and basic strength. However, BaO is toxic and its dissolve in methanol [32]. Hence, the stronger basicity also promotes the transesterification efficiency [33]. Nevertheless, base catalyst is sensitive to FFA and water content which the maximum oil feedstocks with FFA value limited at 2 mg KOH /g. Using of solid base catalyst needs more developed to reduce the deactivation of catalyst and overcome the mass transfer limitation.

2.5 Calcium oxide (CaO)

Calcium oxide (CaO) is an alkaline earth metal oxide which has widely used to catalyze transesterification. CaO is able to produce by thermal composition of calcium carbonate (CaCO₃) at high temperatures as shown in Eq. (2.1) [34]. Most of

research has been usually studied CaO catalyst to produce biodiesel because it provides high catalytic activity, high basic strength, low solubility in methanol and high stability for a longer runs [35]. In addition, advantage of CaO as a solid catalyst can be regenerated and reused. CaO can obtain from renewable source such as eggshell, seashells and animal bones, which has environmentally and economical.



Moreover, calcium oxide (CaO) can be prepared from different calcium sources as calcium nitrate, calcium carbonate, calcium hydroxide and etc. precursors require the different calcination temperature in order to enhance the CaO phase, as seen in Table 2.3 [36].

Table 2.3 Temperature of formation of CaO using various precursors and calcination conditions [36]

| Precursors | Calcination conditions (heating rate, atmosphere) | Formation temperature (°C) |
|-------------------|--|-------------------------------|
| Calcium hydroxide | 1.5 °C/min, N ₂ | 420–650 |
| Calcium hydroxide | 10 °C/min, 20 vol.% O ₂ /Ar | 432-452 |
| Calcium nitrate | 1.5 °C/min, N ₂ | 600 |
| Calcium nitrate | 10 °C/min, 20 vol.% O ₂ /Ar | 633 |
| Limestone | - | 717 |
| Calcium carbonate | 10 °C/min, N ₂ | 614 or 871 |
| Calcium carbonate | Vacuum | 661 |
| Calcium carbonate | 1.5 °C/min, N ₂ | 700 |
| Calcium acetate | >20 °C/min, air | 700 |
| Calcium acetate | 20 °C/min, air | 755 |
| Calcium oxalate | 10 °C/min, 20 vol.% O ₂ /Ar | 800-850 |

2.6 Metal loading catalyst for biodiesel production

The conventional heterogeneous catalyst is usually a single metal such as alkaline metal oxide, transition metal oxide and supported metal. It has been proven to provide the high efficiency for biodiesel production. However, these catalysts might be sensitive to CO₂ atmospheric, water content and FFA, low surface area, required high reaction condition about alcohol to oil, temperature and amount of catalyst and also the deactivation by active sites leaching problem. Co-metal or mixed metal loading catalyst has gained in the number of investigation to enhance catalytic activity, increase surface area and stability [37]. These catalysts are consisting of two or more metal component resulting to obtain the interaction of each metal species and support. This catalyst configuration could increase the basic or acid strength and specific surface area as well as its stability of catalyst [38]. The solid mixed metal oxide can be categorized in 3 types: (1) base, (2) acid and (3) acid-base bifunctional mixed metal oxide catalysts. From above mentioned, the base mixed metal oxide catalysts were used to improve the catalytic performance and stability for transesterification [39]. For instance, high FFA content in oils feedstocks should acid catalyst [40]. Various acid mixed metal oxide catalysts such as WO₃/ZrO₂, TiO₂-SO₄²⁻, etc. In addition, bifunctional mixed metal oxide catalyst can use for simultaneous esterification and transesterification. This advantage of bifunctional catalysts can reduce cost of pre-treat process of biodiesel production [41]. Moreover, based on the reaction rate of acid catalyzed transesterification which was 4,000 times lower than that of base catalyst. Therefore, the selection of mixed metal catalyst for transesterification should be further explored.

2.7 Extruded catalyst

Extrusion is widely used process for shaping material in many fields, including catalyst, agriculture, food and pharmaceutical application. Extrusion was carried out the paste is passed through various die shape to control extruded shape [42]. For catalyst application, extrusion process should be wet paste with using additive, binder and pore forming agent for molding catalyst and support. General, the

additive using in extrusion catalyst was clay or starch, while binder such as alumina, kaolin and diatomite etc. Various factors have effect to shape of extrudates, for example high viscous pastes can block the extruder, while low viscous paste leads to unstable extruded catalyst [43].

The extruded catalysts were obtained attention for continuous process to overcome of several problems including of high pressure drop, clogged and trouble to separation derived from power catalyst. However, the catalytic efficiency of power catalyst is usually higher than that of the extruded catalyst due to its smaller particle size catalyst resulting to reduce internal and external of mass transfer. Therefore, the increase in the catalytic activity of the extruded catalyst is challenge especially for biodiesel production.

2.8 Mass transfer for heterogeneous catalyst

Mass transfer limitations has a role key on rate of reaction. In catalytic reaction, homogeneous catalyst is in a similar phase of reactant, catalyst and product. Thus, mass transfer limitation of homogeneous catalyst between each phase can be negligible. In another hand, heterogeneous catalyst is different phase from substances. Usually, it is a solid phase while reactant and product would be liquid or gas phases. Consequently, reaction rate can be obstacle from mass transfer between phases. The reaction of solid catalyst is taken place on active sites which must be diffused through insides catalyst's pore as shown on Figure 2.4.

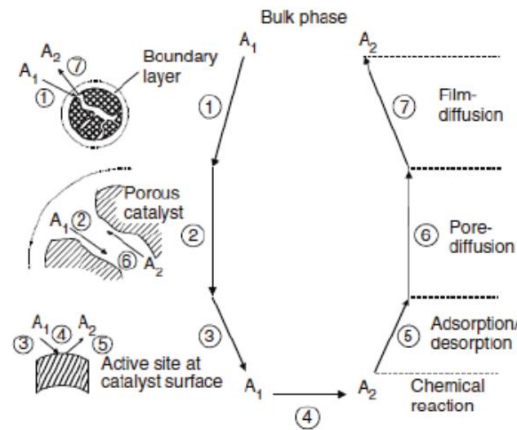


Figure 2.4 Individual steps of a simple, heterogeneous catalytic fluid–solid reaction [44].

Heterogeneous catalysis reaction composes of the 7 steps as following [44].

- (1) Mass transfer of reactant from boundary layer to the external surface of particle
- (2) Molecular diffusion from external surface through interior pore structure.
- (3) Absorption (chemisorption) of reactants at the catalyst surface
- (4) Reaction at specific active sites on the surface
- (5) Desorption of products from interior surface of the catalyst
- (6) Transfer products from interior pore structure to external surface by diffusion
- (7) Mass transfer of products from external surface to boundary layer

2.9 Literature reviews

To develop the efficiency of heterogeneous catalyzed biodiesel forming reaction, there are 2 parts consisting of (1) catalyst forming and (2) metal loading on catalyst.

2.7.1 Catalyst forming

Catalytic processes in industry are usually employed the heterogeneous catalysts. However, the solid catalysts for biodiesel production are still required the development of shaping catalyst instead of using small and fine particle size as

presented in the numerous researches. The small and fine particle catalyst could be limited for using in industry scale [45]. The utilization of pellet catalyst is one of a practical choice to powder catalyst due to easy to separation from reaction mixture and minimize pressure drop for the continuous process. Therefore, the studies of catalyst forming research for biodiesel production are reviewed as following:

Dalibor et al. [9] synthesized CaO loaded on spherically shaped γ -Al₂O₃ catalyst to produce biodiesel from sunflower oil. The catalyst was prepared by impregnation method which was in 1-3 mm diameter. The highest biodiesel yield of 94.3% was obtained under the temperature of 60 °C, methanol to oil molar ratio of 12:1, CaO catalyst loading (based on oil) of 0.5%, stirring rate of 900 rpm and reaction time of 5 h. The catalytic lifetime was only 2 cycles because the mechanical erosion occurred by stirring speed and active site was blocked by organic molecule of reaction mixtures.

Fu et al. [46] studied the effect of various binders, pore-forming agents and calcination temperature for synthesis the extruded CaO-based catalyst. The extruded catalyst was using diatomite, kaolin and activated alumina as binders, while pore-forming agents were polyacrylamide, activated carbon, and polyethylene glycol. The calcination temperature was 700, 800 and 900 °C. This result found that using mass ratio 3:1 of CaO, activated alumina, 3 wt.% of polyacrylamide and calcination temperature 800 °C for transesterification of glycerol and diethyl carbonate. The high catalytic activities of 95.4% glycerol conversion and catalytic stability with consecutive 5 cycles reusability were achieved.

Junior et al. [47] prepared K₂CO₃/ γ -Al₂O₃ by impregnation method using boehmite binder. Various shapes were boehmite powder, boehmite hollow cylinder (5 mm external and 2 mm internal diameter) and boehmite solid cylinder (1.83 mm diameter). These catalysts were soaked in the K₂CO₃ potassium solution for 4 h and calcined at 500 °C for 4 h to obtain γ -Al₂O₃ structure. The high biodiesel yield of 99.3% with using high reaction temperature of 80°C, 4 h reaction time, 5 wt.% of catalyst and 12:1 ethanol to oil molar ratio.

2.7.2 Metal loading on catalyst

Mostly, studied of base metal and mixed-metal oxide loading in heterogeneous catalyst for transesterification due to it can be carry out under mild conditions and faster reaction rate than that of acid mixed-metal oxide. Especially, CaO-, Li₂O-, K₂O- and SrO-based mixed metal oxide catalysts have much attention due to their excellent catalytic performance for biodiesel production. Therefore, the previous research works were summarized as following.

Anastopoulos et al. [48] studied Sr(NO₃)₂/CaO catalyst. The various Sr(NO₃)₂ loading onto CaO catalyst by impregnation method for 24 h to ensure Sr(NO₃)₂ diffused in CaO surface and calcined at 750 °C in air for 6 h. The 35 wt.% of Sr(NO₃)₂ loaded on CaO catalyst gave the best catalytic activity in transesterification with methanol to oil molar ratio of 12:1, a reaction time 2 h, catalyst amount of 3.5 wt.% and stirring speed 600 rpm with 97.3% oil conversion

Palitsakun et al. [49] doped SrO on CaO catalyst derived from waste eggshell to catalyze transesterification of Jatropha oil with methanol. The SrO doping was prepared by wet impregnation method. It was found that methyl ester content of 99.71% using a large methanol to oil ratio of 27.6:1, 65 °C, 89.8 min and 4.77 wt.% of catalyst. The catalytic activity was improved by using SrO/CaO catalyst with 7 mmol of SrO doping. The basicity between CaO and SrO/CaO has been increasing from 6.72 to 13.27 mmol/g.

Al-Saadi et al. [50] have synthesized SrO-ZnO/Al₂O₃ bi-functional catalyst by wet impregnation method for biodiesel production. The bifunctional of SrO-ZnO/Al₂O₃ solid catalysts were various amount of Sr:Zn molar ratio and different calcination temperature. The catalytic activity of 2.6SZA at calcination temperature 900 °C showed the high conversion of 95.1% for biodiesel production under transesterification conditions of 10:1 ethanol to oil molar ratio, 10% catalyst loading, 70 °C and reaction time at 180 min. Moreover, binary oxide (SrO-Al₂O₃) phases can improve catalytic activity in transesterification.

Boro et al. [51] prepared Li₂O doped on CaO eggshell catalyst by impregnation method. The 2% Li loading was an optimum condition to enhance

catalytic activity in transesterification from Nahor oil (non-edible oil) where carried out under 65 °C, 4 h reaction time, 10:1 of methanol to oil molar ratio, using 5 wt.% of catalyst and maximum conversion of 94%.

Lui et al [52]. studied $\text{MgFe}_2\text{O}_4@\text{CaO}$ catalyst via transesterification on soybean oil with methanol. The $7\text{MgFe}_2\text{O}_4@\text{CaO}$ catalyst gave the maximum biodiesel yield of 98.3 % under optimum conditions of 12:1 methanol to oil molar ratio, 70 °C, 3 h reaction time and using catalyst 1 wt.%. The highest basic content was achieved from $7\text{MgFe}_2\text{O}_4@\text{CaO}$ catalyst derived from the interaction of calcium and magnesium mixed metal species. Moreover, magnetic property of iron can assist to separate and recovery, resulting to provide high catalytic reusability within 5 cycles.

Yahaya et al. [53] doped K_2O on dolomite ($\text{MgCa}(\text{CO}_3)_2$) catalyst for FAME production derived from palm oil. K_2O doped on dolomite by impregnation method with various amount of K_2O in range of 5-10 wt.%. Using 15 wt.% K_2O /dolomite, 99% FAME was produced at reaction temperature of 60 °C, 12:1 methanol to oil molar ratio, 1 h reaction time and 1 wt.% of catalyst. In addition, the high basicity of doped catalyst resulted in high catalytic activity. These catalysts were reused for 6 cycles with minor decreased in activity due to the slightly K^+ leaching.

Sulaiman et al. [54] investigated $\text{Cu/Zn}/\gamma\text{-Al}_2\text{O}_3$ catalyst for biodiesel production by impregnation method on the base catalyst. $\text{Cu/Zn}/\gamma\text{-Al}_2\text{O}_3$ catalysts were calcined at 800 °C for 5 h. The Cu played a key role in transesterification. Cu doped on $\text{Zn}/\gamma\text{-Al}_2\text{O}_3$ support can increase the basic properties and surface area by reducing the particle size. The $\text{Cu/Zn}(10:90)/\gamma\text{-Al}_2\text{O}_3$ gave the maximum FAME yield of 90 % with 65 °C, 2 h for reaction time and methanol to oil molar ratio of 20:1 with 10 wt.% of catalyst. The leaching problem of metal loading was a drawback of this catalyst.

CHAPTER 3

EXPERIMENTAL

3.1 Chemicals

A powder activated alumina (Al_2O_3 , MW 101.96 g/mol, melting point of 2,040 °C, pore size 58 Å), guar gum powder and silica sol were obtained from Sigma-Aldrich Chemical Co., Ltd. Calcium carbonate was obtained from Kemaus (Australia) Co., Ltd. Strontium nitrate ($\text{Sr}(\text{NO}_3)_2$, MW 211.63 g/mol) was obtained from Daejung Chemical, Lithium nitrate (LiNO_3), Potassium nitrate (KNO_3), Iron (III) nitrate ($\text{Fe}(\text{NO}_3)_3 \cdot 9\text{H}_2\text{O}$), Morakot palm oil was obtained from Morakot industries public company limited, Thailand. The chemicals used in this research are shown in Table 3.1.

Table 3.1 Specification of chemical in research

| Chemicals | Formula | Molecular weight | Company |
|---------------------------------|--|--------------------|--|
| Calcium carbonate | CaCO_3 | 100.5 g/mol | Kemaus (Australia) Co., Ltd. |
| Activated alumina | Al_2O_3 | 101.96 g/mol | Sigma-Aldrich Chemical Co. Ltd. |
| Guar gum powder | $\text{C}_{10}\text{H}_{14}\text{N}_5\text{Na}_2\text{O}_{12}\text{P}_3$ | 535 g/mol | Sigma-Aldrich Chemical Co. Ltd. |
| Silica sol of 24% concentration | $\text{SiO}_2 \cdot n\text{H}_2\text{O}$ | $60 + n(18)$ g/mol | Sigma-Aldrich Chemical Co. Ltd. |
| Polyacrylamide | $-\text{CH}_2\text{CH}(\text{CONH}_2)-$ | 5.0 g/mol | Apex chemicals Co., Ltd. |
| Strontium nitrate | $\text{Sr}(\text{NO}_3)_2$ | 211.63 g/mol | Daejung Chemical and Materials Co.,Ltd |
| Lithium nitrate | $\text{Li}(\text{NO}_3)$ | 68.95 g/mol | Apex chemicals Co., Ltd. |
| Potassium nitrate | KNO_3 | 101.11 g/mol | Univar solutions Co., Ltd. |
| Iron (III) nitrate | $\text{Fe}(\text{NO}_3)_3 \cdot 9\text{H}_2\text{O}$ | 404 g/mol | Kemaus (Australia) Co., Ltd. |

3.2 Procedure for catalyst preparation

The CaO/Al₂O₃ pellet catalyst was prepared as follows: Al₂O₃ powder was dried at 100°C for 12 h to remove water. After that, the desired amounts of calcium carbonate, guar gum powder and 1 wt.% of polyacrylamide were mixed adequately. Then, the silica sol was added to the powder mixture as a paste form. The mixture was loaded into a load frame machine and compressively pressed to form the CaO pellet catalyst as a short cylindrical shape of 3 mm in diameter and 1.5 mm in length. The pellet catalyst was dried at 100°C for 2 h. After that, the 20 wt.% of metal loading on CaO/Al₂O₃ (M-CaO/Al₂O₃) pellet catalyst was prepared using the incipient wetness impregnation method of an aqueous solution on CaO/Al₂O₃ pellet catalyst for 24 h before calcination at 800°C for 5 h.

3.3 Catalytic activity test

The activities of the catalysts were measured via transesterification of palm oil with methanol. The catalytic activity performance of M-CaO/Al₂O₃ catalyst was carried out in a 75 mL round bottom 3-necks glass flask fitted with a reflux condenser and a thermometer. The reaction temperature was controlled using a silicon oil bath and a hot plate stirrer. In each experimental run, the pellet catalyst and methanol were firstly mixed in the flask at room temperature for 60 min. Then, preheated palm oil was added to the mixture at the reaction temperature to start the reaction. The molar ratio of methanol to palm oil was fixed at 12:1, 10 wt.% of catalyst loading, at the temperature of 65°C, for 6 h using a stirring speed of 600 rpm [55]. The liquid sample was taken on the reaction period; 0, 0.5, 1, 2, 4 and 6 h. The liquid reaction mixture was taken out from the 3-necks glass flask and sampled to analyze the FAME yield using EN 14103 standard.

3.5 Catalyst characterization

3.5.1 Thermogravimetric analysis/differential scanning calorimeter (TGA/DSC)

Thermal stability of uncalcined CaO pellet catalysts was analyzed by thermogravimetric analysis with differential scanning calorimeter (TGA/DSC, SDT Q600

Diamond Thermogravimetric and Differential Analyzer, TA Instruments). The analysis was operated from room temperature to 1000°C at a heating rate of 10°C/min using 100 mL/min of air zero.

3.5.2 X-ray diffraction (XRD)

Crystallinity and phase of catalysts were characterized by XRD (Bruker D8 Advance, Cu K α at 0.154056 nm) between 10° and 80° with a step size of 0.04° and a scan rate of 0.5 s per step.

3.5.3 Scanning electron microscope and energy dispersive X-ray spectrometer (SEM/EDX)

Surface morphology and elemental composition of the single metal loading CaO/Al₂O₃ pellet catalyst were analyzed with scanning electron microscope equipped (SEM) by JEOL JSM-35 the SEM model S3400N and Link Isis Series 300 program Apollo model x is performed for EDX.

3.5.4 Fourier-transform infrared spectroscopy (FTIR)

FTIR-ATR spectra were recorded using the Perkin-Elmer® Spectrum TM 400 FT-IR/NIR spectrometer (Perkin Elmer Inc., Tres Cantos, Madrid) in mid-IR mode, equipped with a universal attenuated total reflectance (ATR) sampling device containing diamond/Zn-Se crystal. The spectra were scanned at room temperature in absorbance mode over the wavenumber range of 4000–650 cm⁻¹, with a scan speed of 0.20 cm/s, and 30 accumulations a resolution of 4 cm⁻¹.

3.5.5 Hammett indicators

Hammett indicator method was used to determine the basicity and basic strength of the synthesized catalyst using three indicators including of bromothymol blue (H_a=7.2), phenolphthalein (H_a=9.8) and 2, 4-dinitroaniline (H_a=15.0). Pellet catalysts were crushed 0.3 g, their crushed catalysts were added into methanol 10 mL and hold for 2 h to reach equilibrium. The clear solution was obtained from filtration. The selected indicator was dropped in the clear solution to test the basic strength. After that, for the clear solution was titrated with benzoic acid 0.1 M to determine the basicity concentration.

3.5.6 CO₂ temperature programmed desorption of carbon dioxide (CO₂-TPD)

The basicity of catalyst was also measured by using temperature programmed desorption of carbon dioxide using Micromeritics Chemisorb 2750 automated system. The determination of basicity was following by the 0.05 g catalyst was loaded and pretreated with carrier flow 25 mL/min at 250 °C for 30 min. Then, adsorbed CO₂ at 30 °C for 1 h. and heated up to 850 °C by heating rate of 10 °C/min.

3.5.7 N₂ adsorption–desorption isotherms by using Brunauer-Emmett-Teller method (BET)

Surface area, pore volume and average pore size were analyzed by N₂ adsorption-desorption with micromeritics ASAP 2020. All samples were crushed and degassed before the test under vacuum at 200 °C for 12 h. The surface area was calculated with Brunauer-Emmett-Teller (BET) model, while the pore volume and pore size were calculated by Barrett-Joyner-Halenda (BJH) model.

3.5.8 Mechanical strength

Mechanical testing equipment by Load frame machine has been used to measure the mechanical strength of the pellet catalyst pellets. The individual pellet catalyst particle was placed on the test bench during the testing. The pellet catalyst particle was broken by applying the desired force. The tester generated the force-time curve on its own. As a result, the maximum force that the particle sample could endure. To achieve an average strength value, at least three tests were done for each pellet catalysts.

3.5.9 Biodiesel (FAME) production analysis using gas chromatography according to EN 14103 standard

3.5.9.1 Standard solution of methyl heptadecanoate was weighed to 0.05 ± 0.0005 g in a 5 mL brown bottle.

3.5.9.2 Reaction mixture samples were weighed to 0.0250 ± 0.0015 g, 5 mL heptane using pipette. Close the lid immediately and shake to allow the solution to be mixed. Then, the sample solution was injected in the amount of 1 μ L. Biodiesel (FAME) content obtained from transesterification of palm oil was then analyzed using gas chromatography using a DB-WAX column (30 m \times 0.320 mm, 0.25

μm) starting at a temperature of 150°C with a holding time of 5 min. Then, the temperature was increased to 190°C at 3°C/min and held for 5 min. Finally, the temperature was increased to 220°C at 3°C/min and held for 5 min. FAME yield was calculated using Eq. (3.1). Free fatty acid methyl ester (FAME) was determined as presented in Table 3.2 according to EN14103.

$$\text{FAME yield (\%)} = \frac{\sum A_{\text{FAME}}}{A_{\text{Ref}}} \times \frac{m_{\text{Ref}}}{m_{\text{FAME}}} \times 100\% \quad (3.1)$$

where A_{FAME} , A_{Ref} , m_{Ref} and m_{FAME} refer to the area of FAME, area of biodiesel standard, mass of FAME (g) and mass of biodiesel standard (g), respectively obtained by gas chromatography analysis.

Table 3.2 conditions of gas chromatography analysis to determine free fatty acid methyl ester (FAME)

| Parameters | Condition |
|--------------------------|-----------------|
| Injection port | |
| Injection mode | Split |
| Carrier gas | He |
| Temperature | 250°C |
| Pressure | 99kPa |
| Injection volume | 1 μL |
| Column oven | |
| Initial temperature | 150°C |
| Total program time | 22 min |
| Ramp rate | 10°C/min |
| Zone 1 | 150°C hold 5min |
| Zone 2 | 190°C hold 5min |
| Zone 3 | 220°C hold 5min |
| Column final temperature | 220°C |

3.5.10 The initial turnover frequency (TOF, time^{-1}) was calculation by using the initial rate and total basicity as followed by Eq. (3.2) [56].

$$\text{The initial TOF (time}^{-1}\text{)} = \frac{\text{Initial rate of oil consumption}}{\text{total basicity of catalyst}} \quad (3.2)$$

where the initial rate of oil consumption is in mmol/mL-g cat and total basicity is in mmol/g cat . The calculation of initial rate and initial TOF obtained from all pellet catalysts were expressed in Appendix D.



CHAPTER 4

RESULTS AND DISCUSSION

4.1 Catalyst characterization of metal doped on CaO/Al₂O₃ pellet catalysts

4.1.1 Thermogravimetric analysis/differential scanning calorimeter (TGA/DSC)

Thermogravimetric analysis/differential scanning calorimeter (TGA/DSC) was carried out to determine the thermal properties of different metal doped on CaO/Al₂O₃ pellet catalysts to determine a suitable calcination temperature of catalyst in range 30 to 1000 °C as shown in Figure 4.1.

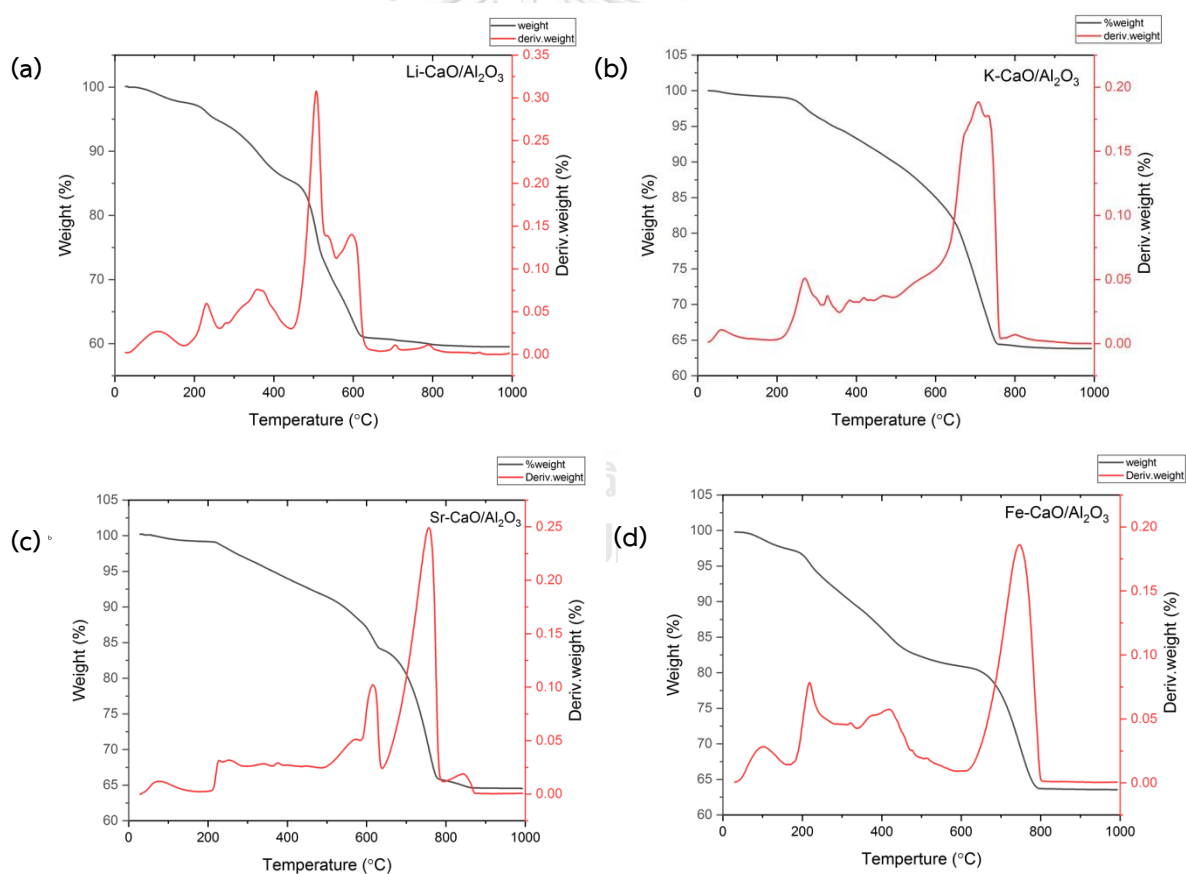


Figure 4.1 Thermogravimetric analysis/differential scanning calorimeter (TGA/DSC) of different metal doped on CaO/Al₂O₃ pellet catalysts

(a) Li-CaO/Al₂O₃, (b) K-CaO/Al₂O₃, (c) Sr-CaO/Al₂O₃, (d) Fe-CaO/Al₂O₃

All uncalcined metal loading on CaO/Al₂O₃ pallet catalysts composed 3 major ranges of weight loss including the first 0.7-0.9% occurring at temperature below 200 °C due to removal of moisture. When temperature increased from 200 to 450 °C, the second weight loss step of 6.5-12.1% expressed the decomposition of silica sol and guar gum powder [46]. The last stage as a major weight loss of 21-24.8% was due to conversion of CaCO₃ to CaO at temperature about 750 °C as corresponding to DTA curve. This can confirm the endothermic reaction of CaCO₃ decomposition. The selected metal oxide loading on the CaO/Al₂O₃ pallet catalyst found the weight loss from the decomposition of nitrate precursor. For instance, Figure 4.1 (a) presents the thermogravimetric results of Li-CaO/Al₂O₃ catalyst, it was found 1.1% weight loss at 234 °C while a large weight loss of 21.9% at the temperature about 500-600°C of LiNO₃ was obtained due to the decomposition to Li₂O [57, 58]. Figure 4.1 (b) shows the thermogravimetric results of K-CaO/Al₂O₃ catalyst, only 3.6% weight loss was in the temperature range of 300-330 and large amount of weight loss was observed at 765 °C corresponding to melting point of KNO₃, and KNO₂ decomposition into K₂O, respectively [59]. Figure 4.1 (c) illustrates 9.1 % weight loss of Sr-CaO/Al₂O₃ catalyst in the temperature range of 560-615 °C corresponding to the SrNO₃ decomposition to SrO [50]. In addition, 10.4% weight loss of Fe(NO₃)₃·9H₂O of Fe-CaO/Al₂O₃ catalyst was found the decomposition at 200-400°C to Fe₂O₃ as indicated in Figure 4.1 (d) [60]. The above results demonstrated that the decomposition temperature to generate oxide catalyst for all catalyst precursors were less than 800 °C. Therefore, the selected calcination temperature of 800 °C should be appropriate for the preparation of these catalyst pellets.

4.1.2 X-ray diffraction (XRD)

XRD patterns and crystalline structures of CaO/Al₂O₃ pellet catalysts with different metal doping and bare CaO/Al₂O₃ pellet catalyst are shown in Figure 4.2.

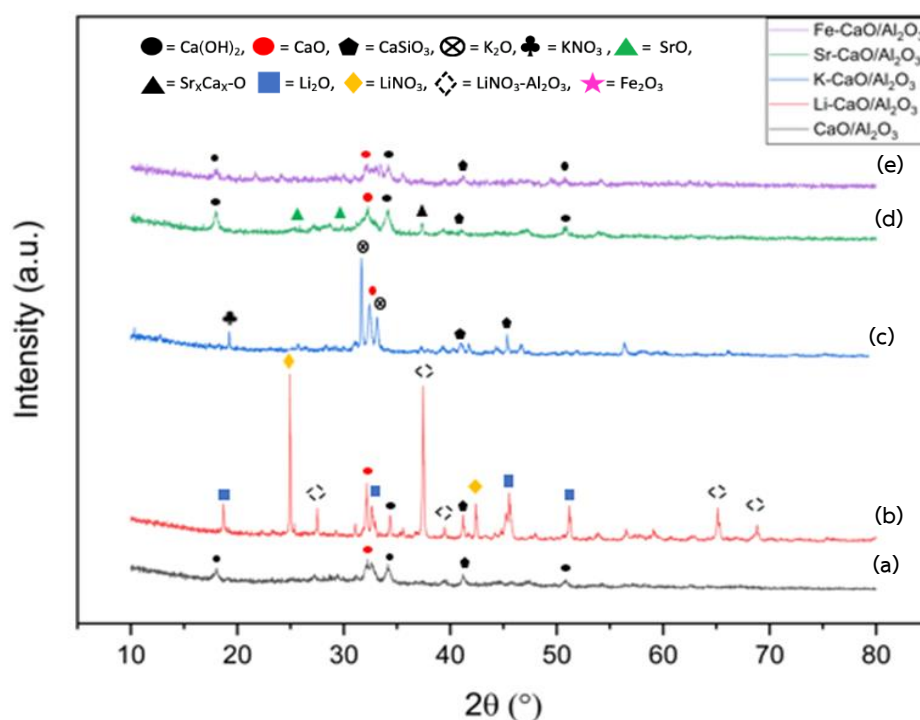


Figure 4.2 X-rays diffraction of different metal doped on $\text{CaO}/\text{Al}_2\text{O}_3$ pellet catalysts (a) $\text{CaO}/\text{Al}_2\text{O}_3$ (b) $\text{Li-CaO}/\text{Al}_2\text{O}_3$ (c) $\text{K-CaO}/\text{Al}_2\text{O}_3$, (d) $\text{Sr-CaO}/\text{Al}_2\text{O}_3$ and (e) $\text{Fe-CaO}/\text{Al}_2\text{O}_3$,

Figure 4.2 shows the XRD patterns of different single metal doped on $\text{CaO}/\text{Al}_2\text{O}_3$ pellet catalysts. The peak of CaO was appeared (at $2\theta = 32.26^\circ$ and 50.84°) as an active phase for all single metal doped on $\text{CaO}/\text{Al}_2\text{O}_3$ pellet catalysts. The XRD pattern of Ca(OH)_2 was also observed at $2\theta = 17.98^\circ$, 28.90° and 50.71° because the hydration of CaO can occur when catalyst was surrounded by moisture the air [46]. In addition, the formation of new phase was occurred at $2\theta = 41.37^\circ$ and 45.68° [46]. It indicated the presence of CaSiO_3 obtained from the silica sol in the pellet preparation process. Both $\text{Li-CaO}/\text{Al}_2\text{O}_3$ and $\text{K-CaO}/\text{Al}_2\text{O}_3$ pellet catalysts illustrated the dominate and sharp characteristic peaks. The intensity peaks of $\text{Li-CaO}/\text{Al}_2\text{O}_3$ pellet catalyst appeared at $2\theta = 18.48^\circ$, 34.28° , 47.37° and 51.07° were derived from Li_2O [51]. However, it can be seen the lower intensity peaks of LiNO_3 at $2\theta = 25.0^\circ$ and 42.33° [61], and $\text{LiNO}_3\text{-Al}_2\text{O}_3$ at $2\theta = 29^\circ$, 37.8° , 66.5° and 68.6° [62], respectively. Similarly, $\text{K-CaO}/\text{Al}_2\text{O}_3$ catalyst exhibited the XRD pattern at $2\theta = 25.21^\circ$,

28.61°, 31.84° and 40.62° and 55° indicating K₂O crystal including found that KNO₃ phase at 2θ = 19.0° [63]. Meanwhile, Sr-CaO/Al₂O₃ and Fe-CaO/Al₂O₃ were lower intensity peaks which can be attributed their smaller crystallite size. At 2θ = 25.19° and 28.29° related to the SrO phase [64], while Fe₂O₃ phase was occurred at 2θ = 32.93° [65]. Based on XRD pattern of CaO/Al₂O₃ modified with metals loading, this confirmed that each metal oxide phase was incorporated on the CaO/Al₂O₃ pellet catalysts.

The values of crystallite size of CaO and metal oxide loading on CaO/Al₂O₃ pellet catalysts by impregnation method are presented in Table 4.1 which was determined by Debye Scherer equation. The crystallite sizes of CaO were 5.2, 18.1, 26.1, 6.2 and 8.7 nm for CaO/Al₂O₃, K-CaO/Al₂O₃, Li-CaO/Al₂O₃, Sr-CaO/Al₂O₃ and Fe-CaO/Al₂O₃ pellet catalysts, respectively. The crystallite sizes of Ca(OH)₂ were 17.2, 16.9 and 26.2 nm for CaO/Al₂O₃, Sr-CaO/Al₂O₃ and Fe-CaO/Al₂O₃ pellet catalysts, respectively. It was interesting to find that CaO crystallite size derived from K-CaO/Al₂O₃ and Li-CaO/Al₂O₃ pellet catalysts were larger than the others. This might be indicated that the agglomeration of K and Li metal oxide with CaO metal oxide species on the CaO/Al₂O₃ pellet catalysts as the decomposition temperature of nitrate precursor was found to be 234-600 °C which was lower than that of Sr and Fe-CaO/Al₂O₃ pellet catalysts.

Moreover, crystallite sizes of K₂O, Li₂O, SrO and Fe₂O₃ as metal oxide were 45.1, 37.3, 14.8 and 4.9 nm, in respectively. The larger crystallite sizes of metal oxide loading were more likely resulted from a small surface area of catalysts and poor dispersion of metal loading of the CaO/Al₂O₃ pellet catalysts. On the other hand, some sintering effect of K-CaO/Al₂O₃ and Li-CaO/Al₂O₃ metal oxides loading was observed at calcination temperature at 800 °C. Addition of K, Li and other monovalent cations was reported that the calcination temperature could affect particle size [66].

Table 4.1 Crystallite sizes of the different metal oxide species using different metal loading on CaO/Al₂O₃ pellet catalysts

| Catalyst | Crystallite size (nm) | | | | | |
|---------------------------------------|-----------------------|---------------------|-------------------|------------------|------|--------------------------------|
| | CaO | Ca(OH) ₂ | Li ₂ O | K ₂ O | SrO | Fe ₂ O ₃ |
| CaO/Al ₂ O ₃ | 5.2 | 17.2 | - | - | - | - |
| Li-CaO/Al ₂ O ₃ | 18.1 | - | 37.3 | - | - | - |
| K-CaO/Al ₂ O ₃ | 26.1 | - | - | 45.1 | - | - |
| Sr-CaO/Al ₂ O ₃ | 6.2 | 16.9 | - | - | 14.8 | - |
| Fe-CaO/Al ₂ O ₃ | 8.7 | 26.2 | - | - | - | 4.9 |

4.1.3 Fourier-transform infrared spectroscopy (FTIR)

Functional group of CaO/Al₂O₃ pellet catalysts modified by metal oxides (M-CaO/Al₂O₃) and bare CaO/Al₂O₃ pellet catalyst were presented in Figure 4.3. The spectra of O-Ca-O and Si-O-Si were observed at 875.77, 1450 and 2350 cm⁻¹, respectively for all metal oxides on CaO/Al₂O₃ and bare CaO/Al₂O₃ pellet catalysts which was generated from silica sol to assist in the paste formation in the extrusion process [67]. Moreover, the characteristic peak at wavenumber 3642 cm⁻¹ corresponded to the hydroxyl (-OH) vibration for CaO/Al₂O₃ pellet catalyst derived from the moisture adsorption from the air or precursor decomposition except K-CaO/Al₂O₃ and Li-CaO/Al₂O₃ catalysts, corresponding with XRD results. This result was in agreement to the report of Hu et al. [46]. The synthesized KNO₃/CaO catalyst was not found K-OH band (3741 cm⁻¹). In addition, AlSharifi et al. [58] reported that no Li-OH functional group was observed. This might be speculated that using K and Li loading on CaO could prevent the adsorption of moisture on the catalyst surface. A peak at 700 cm⁻¹ represented Li-O while the wavenumber at 1787.33 cm⁻¹ represented Li-Ca interaction as illustrated in Figure 4.3 (b). Figure 4.3 (c) shows the adsorption band of K-O observed at 1433 cm⁻¹ [53]. The Sr-O functional group was observed at 855 and 1446 cm⁻¹ as indicated in Figure 4.3 (d) [41]. Figure 4.3 (e)

indicates wavenumber of Fe-O at 613 and 1039 cm^{-1} were presented as previously observed in the previous report [68]. Therefore, all impregnation of the selected metal on the $\text{CaO}/\text{Al}_2\text{O}_3$ pellet catalysts was successfully prepared.

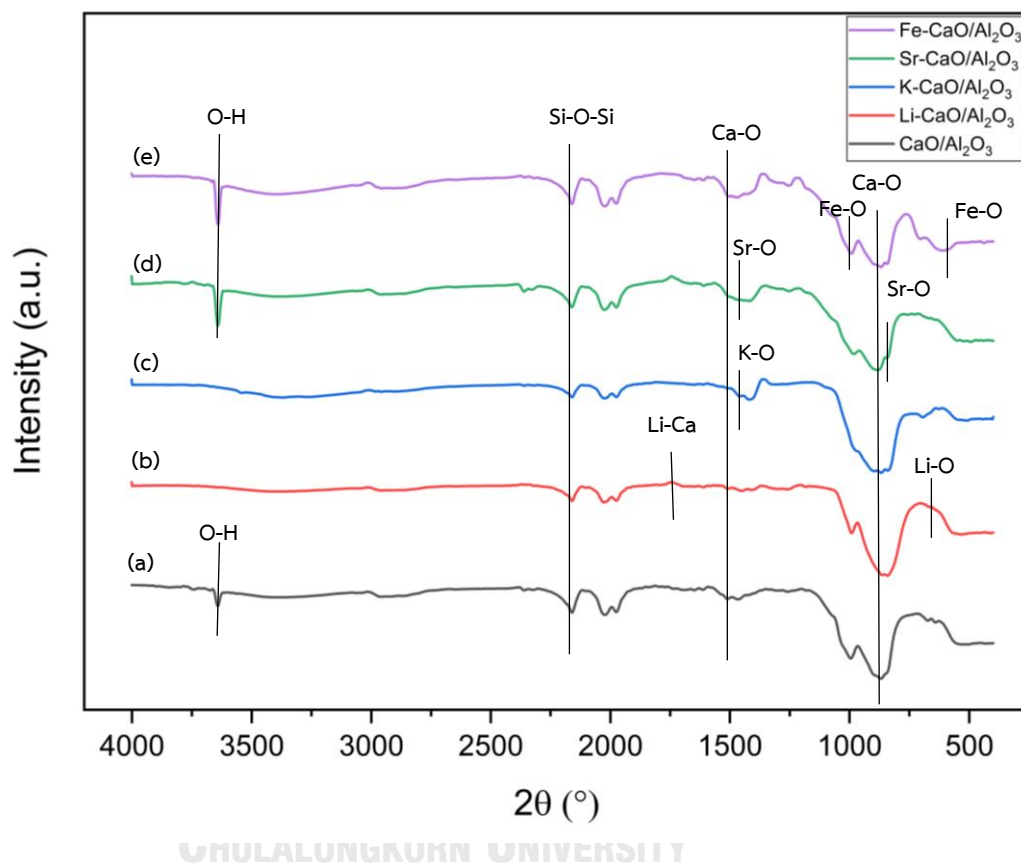


Figure 4.3 Fourier transform infrared spectroscopy (FTIR) of metal doped on $\text{CaO}/\text{Al}_2\text{O}_3$ pellet catalysts using different metal species (a) $\text{CaO}/\text{Al}_2\text{O}_3$, (b) $\text{Li-CaO}/\text{Al}_2\text{O}_3$, (c) $\text{K-CaO}/\text{Al}_2\text{O}_3$, (d) $\text{Sr-CaO}/\text{Al}_2\text{O}_3$, and (e) $\text{Fe-CaO}/\text{Al}_2\text{O}_3$,

4.1.4 Surface morphology of $\text{CaO}/\text{Al}_2\text{O}_3$ pellet catalyst with metal doped using scanning electron microscope and energy dispersive X-ray spectrometer (SEM/EDX)

The surface morphologies and dispersion of metal loading on $\text{CaO}/\text{Al}_2\text{O}_3$ pellet catalyst were investigated using SEM/EDX and summarized in Table 4.2. These images showed the morphology of the pellet catalysts. The particles in the

$\text{CaO}/\text{Al}_2\text{O}_3$ were found an irregular in polygonal of catalyst before doping the selected metal oxide. Lu et al. also suggested that the agglomeration of a particle was decreased by using a pore-forming agent for $\text{CaO}/\text{Al}_2\text{O}_3$ extruded catalyst [46]. The similar shape of $\text{CaO}/\text{Al}_2\text{O}_3$ catalyst was achieved after the single metal oxide was doped for both $\text{Li-CaO}/\text{Al}_2\text{O}_3$ and $\text{K-CaO}/\text{Al}_2\text{O}_3$ pellet catalysts. Meanwhile, $\text{Sr-CaO}/\text{Al}_2\text{O}_3$ pellet catalyst was observed some needle and irregular shapes. For $\text{Fe-CaO}/\text{Al}_2\text{O}_3$ pellet catalyst exhibited a uniform distribution in spherical shape and some irregular shape. In addition, Table 4.2 also presents the distribution of metal oxide doping on $\text{CaO}/\text{Al}_2\text{O}_3$ pellet catalysts. The $\text{CaO}/\text{Al}_2\text{O}_3$ catalyst exhibits uniform dispersion of Ca element as a major composition. The well dispersion on $\text{CaO}/\text{Al}_2\text{O}_3$ pellet catalysts was observed for metal oxide doped, $\text{K-CaO}/\text{Al}_2\text{O}_3$ and $\text{Sr-CaO}/\text{Al}_2\text{O}_3$ catalysts as a promotor except $\text{Li-CaO}/\text{Al}_2\text{O}_3$ pellet catalyst. This should be because the EDX technique could not detect the smallest atom as belong to Li-species [69]. The agglomerate of Fe metal oxide on $\text{Fe-CaO}/\text{Al}_2\text{O}_3$ pellet catalysts was presented in Table 4.2 (f) which could affect its catalytic activity as further discussed in the next section. The average particle size of bare $\text{CaO}/\text{Al}_2\text{O}_3$ pellet catalyst was $0.43 \mu\text{m}$. Meanwhile, metal oxides loading on $\text{CaO}/\text{Al}_2\text{O}_3$ pellet catalysts as $\text{K-CaO}/\text{Al}_2\text{O}_3$, $\text{Li-CaO}/\text{Al}_2\text{O}_3$, $\text{Sr-CaO}/\text{Al}_2\text{O}_3$ and $\text{Fe-CaO}/\text{Al}_2\text{O}_3$ were 0.52 , 0.82 , 0.56 and $0.35 \mu\text{m}$, respectively. This can be confirmed that the agglomeration of crystal as compared to the XRD results.

Figure 4.4 presents the element composition of pellet catalyst by EDS technique. Figure 4.4 (a) presents Ca, Al and O elements of $\text{CaO}/\text{Al}_2\text{O}_3$ pellet catalyst with high dispersion of Ca on Al_2O_3 . Figures 4.4 (b) – (d) shows K, Sr and Fe elements of metal oxides loading on $\text{CaO}/\text{Al}_2\text{O}_3$ pellet catalysts, $\text{Fe-CaO}/\text{Al}_2\text{O}_3$ pellet catalyst were agglomerated on the support surface, agreeing to Fe elements as 29.63% according to EDS results. While K and Sr elements were close to 20 wt.% of metal loading. However, it was rather to follow the synthesis metal loading of 20 wt.% on the $\text{CaO}/\text{Al}_2\text{O}_3$ pellet catalysts.

Table 4.2 Surface morphology of CaO/Al₂O₃ pellet catalysts with metal doped by using scanning electron microscope and energy dispersive X-ray spectrometer (SEM/EDX)

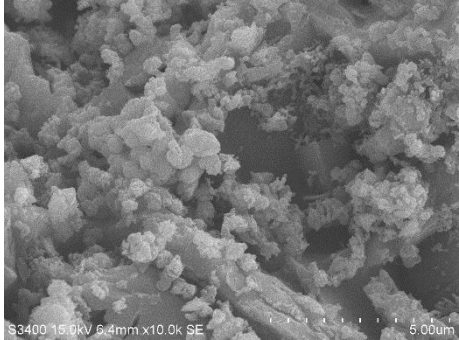
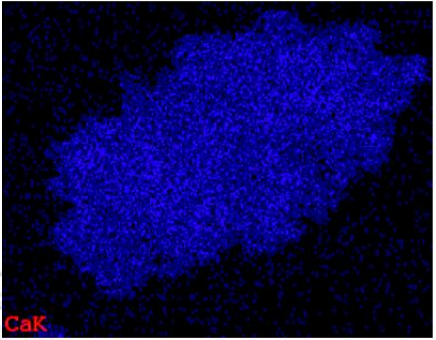
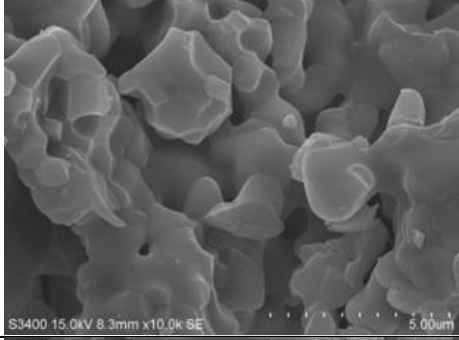
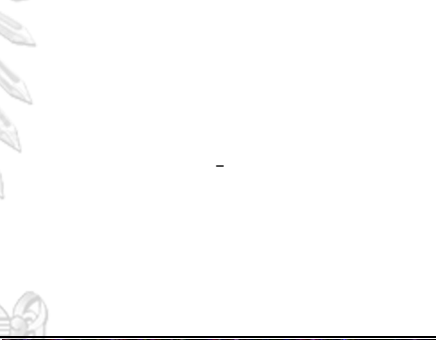
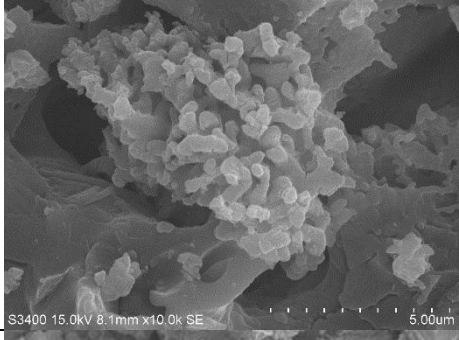
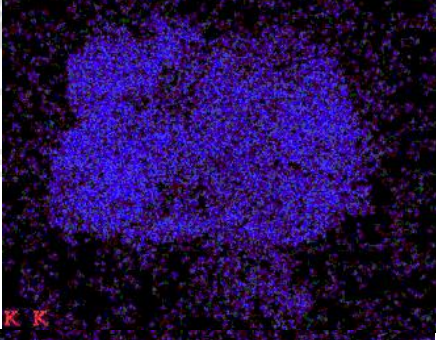
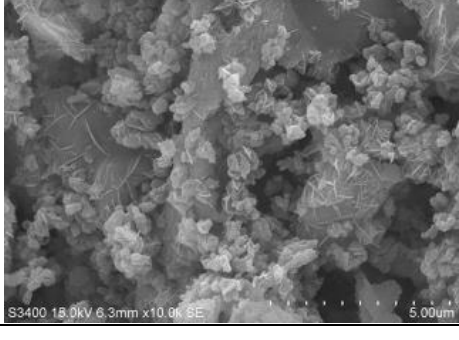
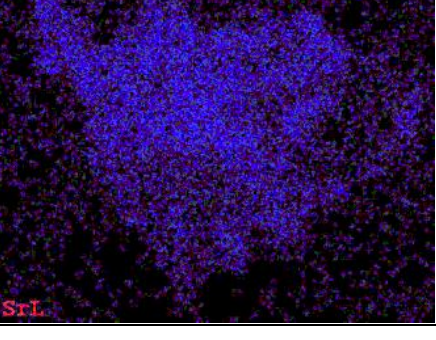
| Catalyst | SEM | Dispersion (metal) |
|---|---|--|
| (a) CaO/Al ₂ O ₃ |  |  |
| (b) Li- CaO/Al ₂ O ₃ |  |  |
| (c) K- CaO/Al ₂ O ₃ |  |  |
| (d) Sr- CaO/Al ₂ O ₃ |  |  |

Table 4.2 Surface morphology of CaO/Al₂O₃ pellet catalysts with metal doped by using scanning electron microscope and energy dispersive X-ray spectrometer (SEM/EDX) (Cont.)

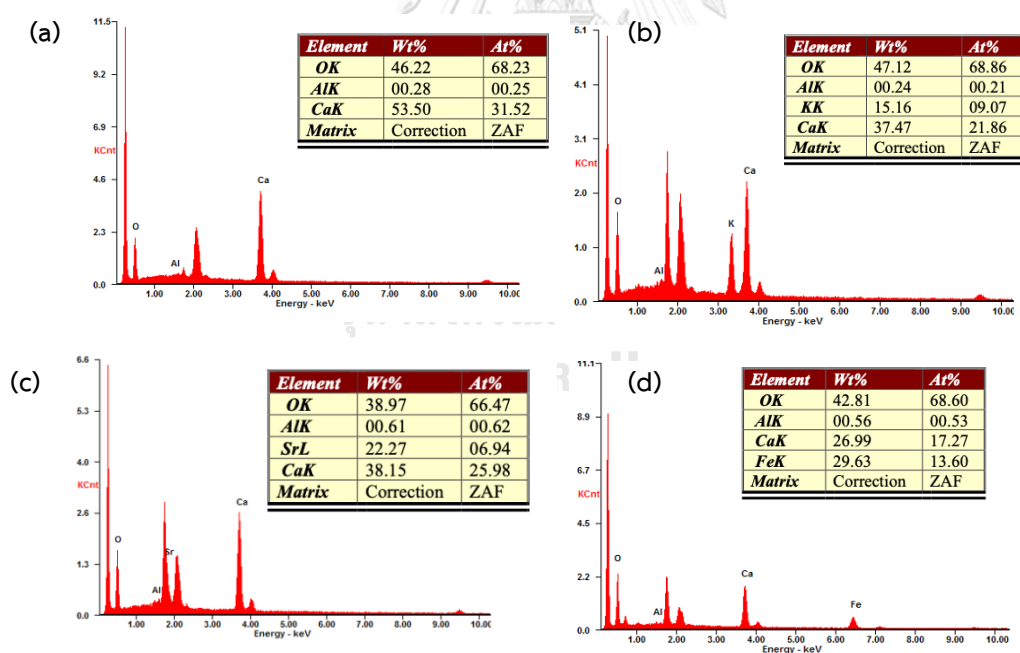
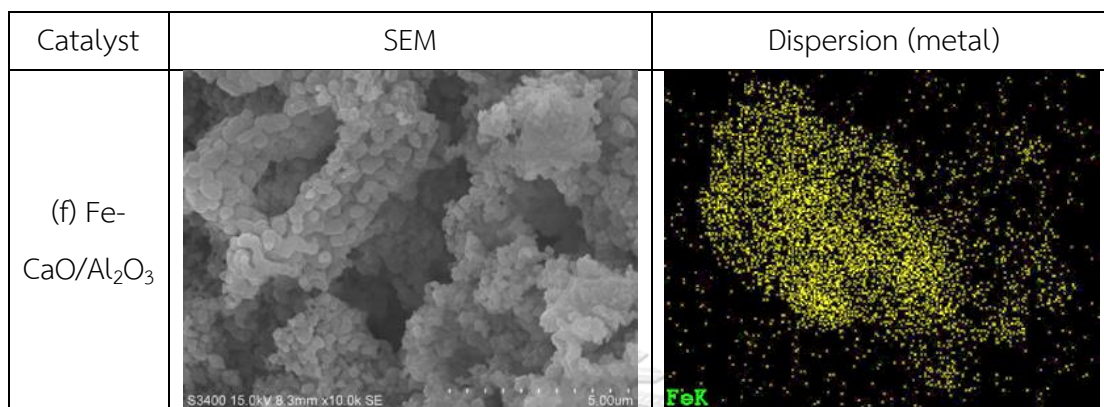


Figure 4.4 The element compositions of metal doped on CaO/Al₂O₃ pellet catalysts using different metal species (a) CaO/Al₂O₃, (b) K-CaO/Al₂O₃, (c) Sr-CaO/Al₂O₃ and (d) Fe-CaO/Al₂O₃

4.1.5 N₂ adsorption–desorption results by using Brunauer-Emmett-Teller method (BET)

BET surface area and average pore size are important textural properties of heterogeneous catalyst which can result in their catalytic activities. The N₂ adsorption–desorption of the synthesized single metal loading on CaO/Al₂O₃ pellet catalysts was illustrated in Table 4.3 and Figures 4.5 - 4.6.

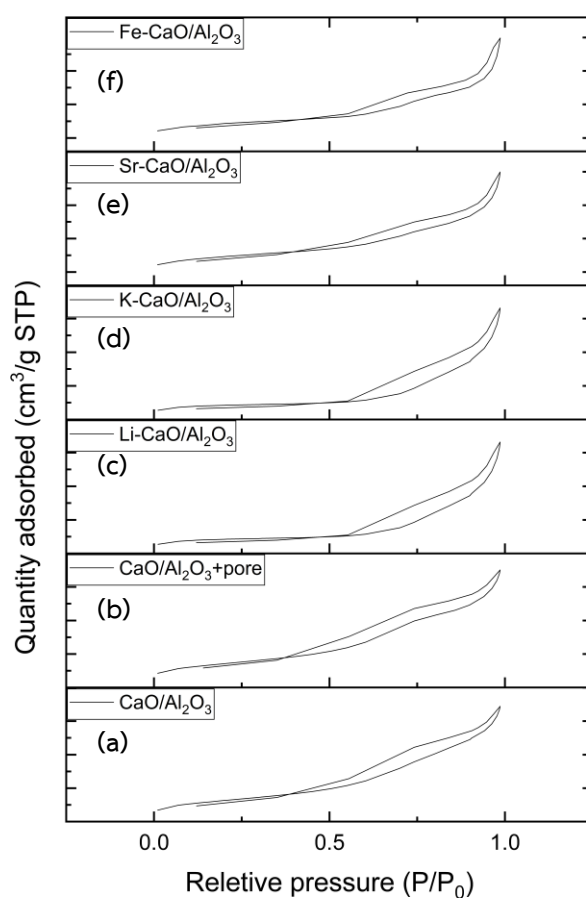


Figure 4.5 Adsorption-desorption isotherms of (a) CaO/Al₂O₃, (b) CaO/Al₂O₃+pore, (c) Li-CaO/Al₂O₃, (d) K-CaO/Al₂O₃, (e) Sr-CaO/Al₂O₃ and (f) Fe-CaO/Al₂O₃ pellet catalysts

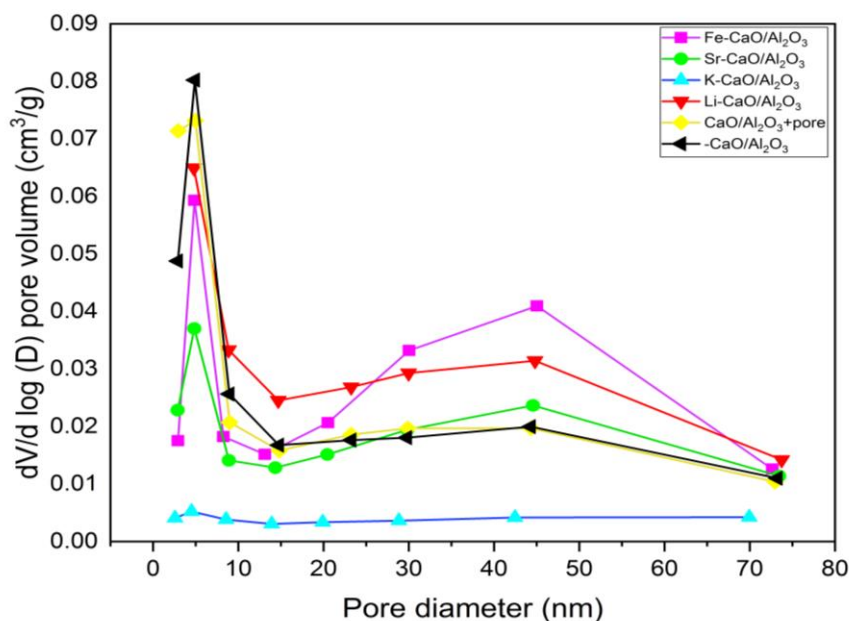


Figure 4.6 Pore size distribution curves of mesoporous (a) CaO/Al₂O₃, (b) CaO/Al₂O₃+pore, (c) Li-CaO/Al₂O₃, (d) K-CaO/Al₂O₃, (e) Sr-CaO/Al₂O₃ and (f) Fe-CaO/Al₂O₃ pellet catalysts

Figure 4.5 presents the adsorption-desorption isotherm of metal oxides loading on CaO/Al₂O₃ pellet catalysts and the bare CaO/Al₂O₃ pellet catalyst. According to the IUPAC classification, all pellet catalysts exhibited the same adsorption-desorption isotherm as type IV, indicating a mesoporous structure. When the relative pressure was greater than 0.4, the amount of N₂ adsorption was increased, suggesting the presence of mesoporous [70]. The pore sizes distribution of metal oxides loading on CaO/Al₂O₃ and bare CaO/Al₂O₃ pellet catalysts were displayed in Figure 4.6. All pellet catalysts show a narrow distribution but, K-CaO/Al₂O₃ pellet catalyst had low distribution due to agglomeration and pore blockage of potassium loading. Yahaya et al. [53] also investigated the pore blocking by potassium loading.

Table 4.3 BET surface area of the CaO/Al₂O₃ pellet catalysts with the single metal doping

| Catalyst | BET surface area (m ² /g) | Average pore diameter (nm) |
|---|---|-------------------------------|
| CaO/Al ₂ O ₃ | 23.37 | 9 |
| Pore forming-CaO/Al ₂ O ₃ | 25.97 | 8 |
| Li-CaO/Al ₂ O ₃ | 14.22 | 13 |
| K-CaO/Al ₂ O ₃ | 5.83 | 6 |
| Sr-CaO/Al ₂ O ₃ | 13.36 | 10 |
| Fe-CaO/Al ₂ O ₃ | 16.27 | 11 |

Table 4.3 shows the specific surface area of bare CaO/Al₂O₃ and metal oxide doping on CaO/Al₂O₃ pellet catalysts determined by the BET technique. To compare CaO/Al₂O₃ and CaO/Al₂O₃ with pore forming agent (polyacrylamide), the CaO/Al₂O₃ pellet catalyst with a pore forming agent of 1 wt.% showed the highest BET surface area of 25.97 m²/g. The higher BET surface area of CaO/Al₂O₃ with pore forming agent than the CaO/Al₂O₃ pellet catalyst is because polyacrylamide as a template could assist to create pores in support on catalyst [46]. For metal oxide doped on CaO/Al₂O₃ pellet catalyst with polyacrylamide, the BET surface area of all metal oxide doping CaO/Al₂O₃ pellet catalysts were decreased for Li-CaO/Al₂O₃, K-CaO/Al₂O₃, Sr-CaO/Al₂O₃ and Fe-CaO/Al₂O₃ as corresponding to 14.22, 5.83, 13.36 and 16.27 m²/g, respectively. For the impregnation of metal on the catalyst support, the large amount of doped metal oxide (20 wt.%) might cover and agglomerate on the catalyst surface resulting in reduction of the surface area. The K-CaO/Al₂O₃ catalyst exhibited the lowest BET surface area due to the pore blockage and a crystallite size of K₂O from XRD result (section 1.4.2), which was in agreement with Yahaya et al. [53]. The K₂O catalyst has only 1.3 m²/g. Zhang et al. [71] prepared SrO-CaO/Al₂O₃ catalyst which has 4.5 m²/g BET surface area. Meher et al. [72] synthesized Li-CaO catalyst by wet impregnation, it was found a BET surface area of 6.9 m²/g. The values of BET surface area of all synthesized single metal loading on CaO/Al₂O₃ pellet

catalyst were higher compared to ones reported in the previous researches. On the other hand, the BET surface of Fe-CaO/Al₂O₃ pellet catalyst was lower than that of Fe-Ca/Al₂O₃ catalyst in a powder form (132.42 m²/g) as reported by Sulaiman et al. [65]. Moreover, heterogeneous catalyst for transesterification should have a larger pore with a diameter of above 5.8 nm, since the biggest molecule as triglycerides reactant can easily diffuse without any diffusion limitations into the active site of solid catalyst [73].

4.1.6 CO₂ temperature programmed desorption of carbon dioxide (CO₂-TPD)

The number of total basic sites of the catalyst is an important factor affecting the catalytic activity performance in transesterification. The CO₂-TPD profiles with different metal loadings on CaO/Al₂O₃ pellet catalysts were illustrated in Figure 4.7. The number of basic sites of catalyst were also presented in Table 4.4.

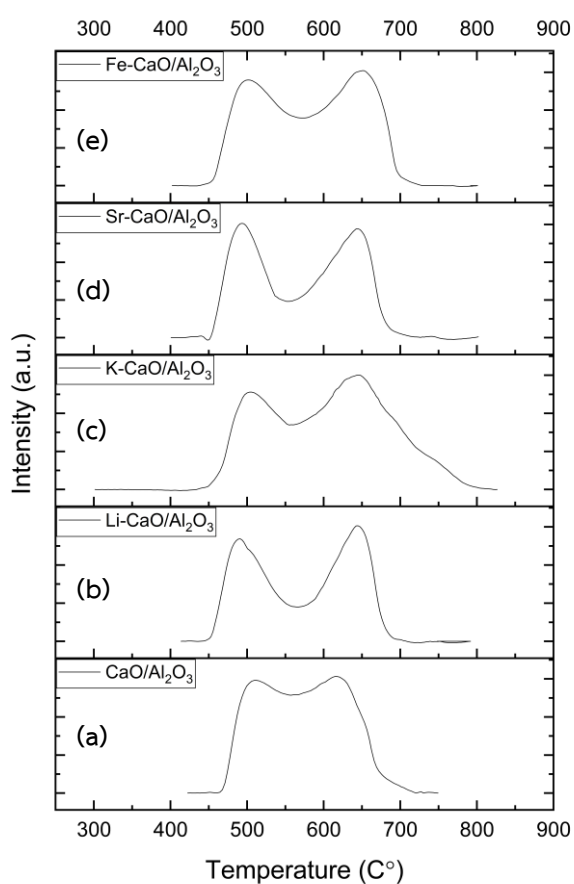


Figure 4.7 CO₂ temperature programmed desorption of carbon dioxide (CO₂-TPD)

of metal doped on CaO/Al₂O₃ pellet catalysts at different species (a) CaO/Al₂O₃, (b) Li-CaO/Al₂O₃, (c) K-CaO/Al₂O₃, (d) Sr-CaO/Al₂O₃ and (e) Fe-CaO/Al₂O₃

The catalysts mainly showed three peaks, each of peak is denoted by the basic sites type and basic strength. The higher temperature of CO₂ desorption could be related to the higher basicity and basic strength. CO₂-TPD spectra of catalysts have been approximately categorized into weak (<200 °C), medium (200-450 °C) and strong (>450 °C) basic sites [74]. Figures 4.6 (a) – (f) showed that all of catalysts possess strong basic site because of their desorbed CO₂ at higher 450 °C. The greater amount of CO₂ adsorbed (higher peak area) on catalyst indicated that the surface catalyst have more basic sites.

Table 4.4 presents the total basicity for CaO/Al₂O₃, Li-CaO/Al₂O₃, K-CaO/Al₂O₃, Sr-CaO/Al₂O₃ and Fe-CaO/Al₂O₃ catalysts being 0.78, 1.49, 2.40, 2.35 and 1.55 mmol/g, respectively. It was explained that the number of basic sites of the catalyst was more likely following the periodic table of elements. When increasing atomic size or energy level in the same group of metal oxides, such as K⁺ > Li⁺ > Na⁺ presented in the same period from right to left of the periodic table, the amount of basicity was also increased. The K-CaO/Al₂O₃ catalyst gave the highest total basicity as 2.40 mmol/g as the potassium oxide has more electron positive in center atom, causing higher basicity. These results are corresponding to report of Lie et al. [75]. They found that the obtained basicity was increased when increasing the ionic radius. This is noteworthy to note that the higher total basicity should offer good catalytic performance for base catalyzed transesterification.

Table 4.4 The number of basic sites of metal loading on CaO/Al₂O₃ pellet catalysts measured by CO₂-TPD

| Catalyst | Weak (mmol/g) | Medium (mmol/g) | Strong (mmol/g) | Total CO ₂ adsorption (mmol/g) |
|---------------------------------------|------------------|--------------------|--------------------|---|
| CaO/Al ₂ O ₃ | - | 0.09 | 0.69 | 0.78 |
| Li-CaO/Al ₂ O ₃ | - | 0.28 | 1.21 | 1.49 |
| K-CaO/Al ₂ O ₃ | - | 0.20 | 2.20 | 2.40 |
| Sr-CaO/Al ₂ O ₃ | - | 0.49 | 1.86 | 2.35 |
| Fe-CaO/Al ₂ O ₃ | - | 0.31 | 1.24 | 1.55 |

4.1.7 Hammett indicators

The basic strength and basicity of different metals loading on CaO/Al₂O₃ and bear CaO/Al₂O₃ pellet catalysts were also shown in Table 4.5. The titration method or the Hammett indicators method were used to determine the basic property of the catalysts with using three indicators including bromothymol blue (H_a=7.2), phenolphthalein (H_a=9.8) and 2, 4-dinitroaniline (H_a=15.0). The result of this method is similar to the CO₂-TPD technique in the section 4.1.6, but using liquid benzoic acid 0.1 M titrated with methanol solution after filtering catalysts and using the selected indicators for the Hammett indicators method. The basic strength of all doped metal CaO/Al₂O₃ pellet catalysts were in range from 7.2 to 9.8 for bromothymol blue (H_a=7.2) and phenolphthalein (H_a=9.8) while 2, 4-dinitroaniline (H_a=15.0) did not appear color changing, indicating the lower the basic strength. The total amount of basicity for CaO/Al₂O₃, Li-CaO/Al₂O₃, K-CaO/Al₂O₃, Sr-CaO/Al₂O₃ and Fe-CaO/Al₂O₃ pellet catalysts were 0.48, 0.13, 0.53, 0.52 and 0.17 mmol/g, respectively which had a similar tendency to the CO₂-TPD approach. The total amount of basicity determined by CO₂-TPD was found to be significantly greater than that determined using the Hammett indicators approach. CO₂-TPD technique using CO₂ as an acid probe to neutralize to the basic site on the catalyst surface which is smaller molecule as a potential to adsorb on all active sites. Moreover, the Hammett indicator technique

determines the soluble basic species in the methanol solution and then titrate with benzoic acid. This indicated that some basic species might not be soluble in methanol to achieve the lower basicity compared to CO₂-TPD technique. However, it can also observe the similar trend of total basicity from these two techniques.

Table 4.5 Basic strength and basicity of metal loading on CaO/Al₂O₃ pellet catalysts measured by Hammett indication method

| Catalyst | Basic strength (H ₊) | Basicity (mmol/g) | | Total basicity (mmol/g) |
|---------------------------------------|-------------------------------------|------------------------|------------------------|----------------------------|
| | | (H ₊ = 7.2) | (H ₊ = 9.8) | |
| CaO/Al ₂ O ₃ | 7.2 < H ₊ < 9.8 | 0.13±0.012 | 0.13±0.035 | 0.27 |
| Li-CaO/Al ₂ O ₃ | 7.2 < H ₊ < 9.8 | 0.10±0.023 | 0.03±0.023 | 0.30 |
| K-CaO/Al ₂ O ₃ | 7.2 < H ₊ < 9.8 | 0.30±0.029 | 0.23±0.047 | 0.53 |
| Sr-CaO/Al ₂ O ₃ | 7.2 < H ₊ < 9.8 | 0.25±0.023 | 0.27±0.011 | 0.52 |
| Fe-CaO/Al ₂ O ₃ | 7.2 < H ₊ < 9.8 | 0.10±0.011 | 0.07±0.001 | 0.17 |

4.1.8 Mechanical strength

The mechanical property test is essential for estimating the catalyst's resistance to breaking during biodiesel production. Usually, these pellet catalysts can collapse because of collision of each other catalysts or the effect of stirrer speed. The synthesized CaO/Al₂O₃ pellet catalyst was used to catalyze liquid phase transesterification, these catalysts were collapsed during transesterification. Therefore, a different metal loading species on CaO/Al₂O₃ pellet catalysts should enhance the mechanical strength of catalyst. After loading the metal oxide on the CaO/Al₂O₃ pellet catalysts, these catalysts should provide a high mechanical strength. Therefore, the mechanical strength of pellet catalysts was investigated as illustrated in Table 4.6.

Table 4.6 Mechanical strength of the bare CaO/Al₂O₃ and metal loading on CaO/Al₂O₃ catalyst.

| Catalyst | Mechanical strength (kN) |
|---------------------------------------|--------------------------|
| CaO/Al ₂ O ₃ | 0.015 |
| Li-CaO/Al ₂ O ₃ | 0.007 |
| K-CaO/Al ₂ O ₃ | 0.017 |
| Sr-CaO/Al ₂ O ₃ | 0.013 |
| Fe-CaO/Al ₂ O ₃ | 0.018 |

The mechanical strength of different metal oxide loading on CaO/Al₂O₃ pellet catalysts were higher than the bare CaO/Al₂O₃ pellet catalyst except Sr-CaO/Al₂O₃ and Li-CaO/Al₂O₃ catalyst pellets. Using 1 wt.% polyacrylamide pore-forming agent in the preparation catalyst process can improve the capability of the pellet catalyst due to cross-linking inside of catalyst [46]. In some report, metal oxide doped can promote the stability of catalyst. Silverira et al. [45] used potassium (K) on the extruded alumina support in biodiesel production. The mechanical strength was increased when amount of potassium (K) was increased from 15 to 35 wt.% including the bimetallic catalyst using iron (Fe) to promote the stability of catalyst [76]. Shi et al. [77] used the CaO@ γ -Fe₂O₃ catalyst for biodiesel production in 4 consecutive times, and more than 80% biodiesel yield was observed, implying its catalytic stability.

4.2 Catalytic activity of CaO/Al₂O₃ pellet catalysts via transesterification of palm oil

4.2.1 Effect of size of CaO/Al₂O₃ pellet catalysts on the catalytic activity of transesterification

Transesterification was employed for biodiesel production at a 12:1 methanol to oil molar ratio at 65 °C using 10 wt.% catalyst, and the biodiesel yield was observed periodically for 6 h reaction time.

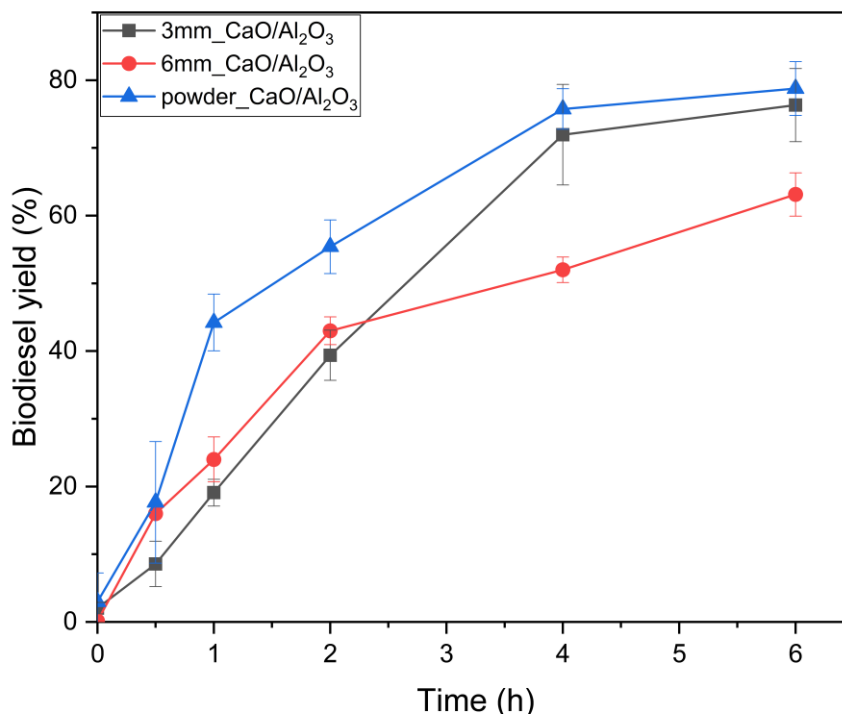


Figure 4.8 Effect of size of CaO/Al₂O₃ pellet catalysts on the catalytic activity of transesterification

Figure 4.8 shows the biodiesel yields along the reaction time using bare CaO/Al₂O₃ pellet catalysts derived from the different diameters of 6 mm and 3 mm with equivalent length and compared to CaO powder catalyst. It was found that the lower biodiesel yields were obtained from the CaO/Al₂O₃ pellet catalysts for both sizes of 3 and 6 mm at the initial transesterification stage compared the CaO powder. This was because the diffusion mass transfer from pellet catalyst was higher than that of power catalyst. However, for 3 mm diameter of pellet catalyst and powder catalyst gave a slightly significant difference in biodiesel yield at 6 h of transesterification as 78.76% and 76.33%, respectively. The biodiesel yield obtained from 6 mm diameter of pellet catalyst was lowest as only 63.12%. The lower specific surface area is corresponding to catalyst with a larger pellet size. This should have an impact on the reaction due to internal mass transfer limitations [78]. Moreover, some pellet at 6 mm diameter of CaO/Al₂O₃ catalyst was broken in first 2 h of reaction

time. This is a reason of initial reaction time of 6 mm diameter had a higher biodiesel yield than that of the 3 mm diameter of CaO/Al₂O₃ pellet catalyst. Witoon et al. [79] studied the effect of catalyst pellet size on the transesterification activity. The biodiesel yield was decreased when using a large pellet size due to internal diffusion limitation phenomena. Thus, CaO/Al₂O₃ pellet catalyst in 3 mm diameter was further used to investigate the effect of single metal loading on the CaO/Al₂O₃ pellet catalysts for transesterification of palm oil.

4.2.2 Effect of CaO/Al₂O₃ pellet catalysts with different metal oxide on the catalytic activity of transesterification

Transesterification was employed for biodiesel production at a 12:1 methanol to oil molar ratio at 65 °C using 10 wt.% catalyst, and the biodiesel yield was observed over 6 h reaction time. Biodiesel yield of the bare CaO/Al₂O₃ pellet catalyst was used to compare with those resulted from Li, K, Sr and Fe loading on CaO/Al₂O₃ pellet catalysts. At the initial transesterification period, it can be seen that the biodiesel yield obtained from the strong base of the metal oxide loading on CaO/Al₂O₃ pellet catalyst was increased. K-CaO/Al₂O₃ pellet catalyst gave the highest biodiesel yield of 95.5% (Figure 4.9,). Meanwhile, the biodiesel yields of Sr-CaO/Al₂O₃, Li-CaO/Al₂O₃, Fe-CaO/Al₂O₃ and CaO/Al₂O₃ pellet catalysts were 91.60, 72.04, 90.28 and 84.26 %, respectively. These results were corresponded to their total basicity. According to Istadi et al. [70], the surface O²⁻ obtains the donor of the H⁺ from CH₃OH and forms CH₃O⁻. This form has a high basicity and high catalytic activity in the transesterification. Although, surface area of the Li-CaO/Al₂O₃ pellet catalyst was rather higher as compared to other metal oxide loading on CaO/Al₂O₃ pellet catalysts. However, this can conclude that the basicity was a remarkable contributing factor in the high biodiesel yield in transesterification. This result was reasonable in agreement with Meher et al. [72] who reported that the surface area has slight effect on transesterification. The order of biodiesel yield at 6 h was corresponded to the basicity of catalyst results as can be found in sections 4.1.6 and 4.1.7. In addition, it can be observed that the K-CaO/Al₂O₃ can decrease the induction period of

transesterification which was corresponding to Kumar and Ali [80]. They found that the K-CaO catalyst gave the high catalytic activity for transesterification of a variety of feedstocks. The complete reaction time was also decreased from 4.5 to 2.5 h using Jathopa oil as a feedstock while using pure CaO catalyst gave only 10% conversion at 10 h of reaction time.

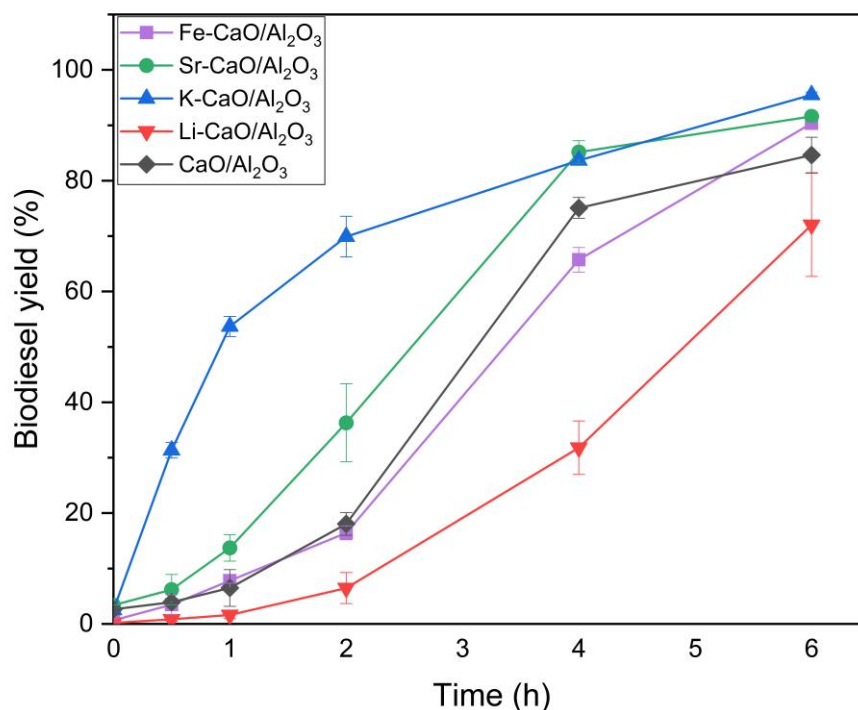


Figure 4.9 Effect of CaO/Al₂O₃ pellet catalysts with different metal oxide on the catalytic activity of transesterification

4.2.3 Effect of CaO/Al₂O₃ pellet catalysts with different metal oxides on the initial rate and initial TOF for catalytic activity of transesterification

The turnover frequency (TOF) is one of the indicators to measure the catalytic reaction performance. The CaO/Al₂O₃ pellet catalysts with different metal oxides were tested the catalytic activity of transesterification under reaction condition at a 12:1 methanol to oil molar ratio at 65 °C using 10 wt.% catalyst after 1 h of reaction time. The initial rate of each biodiesel yield of metal oxide loading on CaO/Al₂O₃ pellet catalysts was determined based on 1 h of transesterification as can

be seen in Figure 4.10. Turnover frequency (TOF) was calculated based on the initial rate and total basicity which measure from CO₂-TPD where the amount of CO₂ adsorbed per unit surface area. Table 4.7 presents the initial rate and initial TOF on CaO/Al₂O₃ pellet catalysts with different metal oxides on the catalytic activity of single metal loading on the CaO/Al₂O₃ pellet catalysts via transesterification. The value of the initial rate is in the unit of mmol/mL-h determined by dividing the number of moles of oil (reactant) consumed under reaction condition (after 1 h) in reaction volume, and the unit of mmol/g cat-h was calculated by dividing the initial rate by catalyst loading in a reaction (mg/mL). It was found that the highest initial rate was obtained for K loading on the CaO/Al₂O₃ pellet catalyst. For the initial TOF, if the proportion of total basicity was higher after calculating the initial TOF, it would reduce the initial TOF. However, the initial TOF of K-CaO/Al₂O₃ pellet catalyst was 0.83 h⁻¹ which was greater than other metal oxide loading on CaO/Al₂O₃ pellet catalyst for transesterification. According to biodiesel yield of K-CaO/Al₂O₃ pellet catalyst at 6 h was 95.5% which was the highest as compared to the others. This can be concluded that K-CaO/Al₂O₃ pellet catalyst was active for transesterification due to the higher basic sites on catalyst surface compared to the others. From the results in the section 4.2.2, K-CaO/Al₂O₃ pellet catalyst can also reduce the induction period in transesterification in which was in agreement to the initial TOF. In contrast, Umdu and Seker [56] reported the initial TOF does not only depend on basicity but also, basic strength should have effect on the initial TOF. However, in this study, the basicity was the key factor to catalyze transesterification based the similar basic strength of metal loading on CaO/Al₂O₃ pellet catalysts.

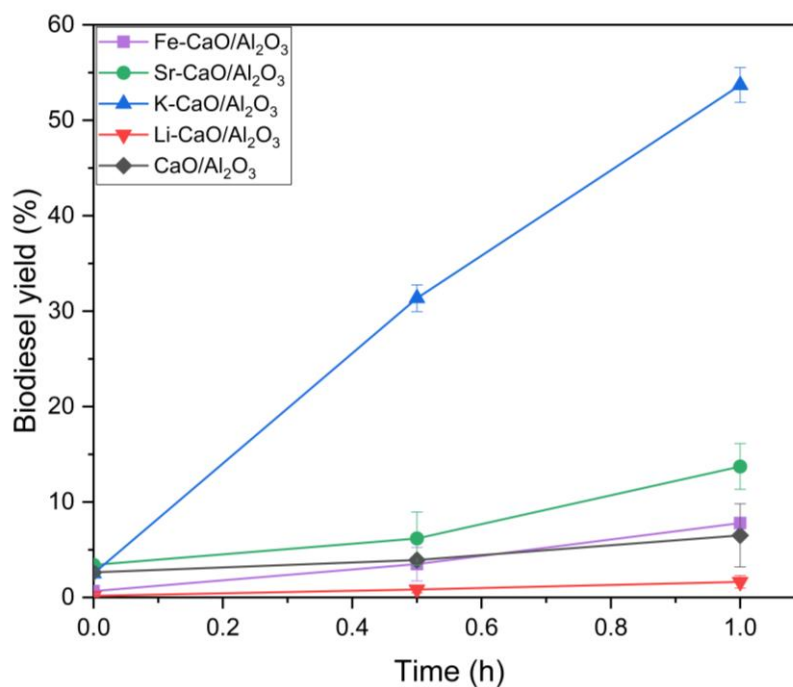


Figure 4.10 Biodiesel yield after 1 h reaction time with different metal oxide loading on the CaO/Al₂O₃ pellet catalysts.

Table 4.7 Initial TOF on CaO/Al₂O₃ pellet catalysts with different metal oxides on the catalytic activity via transesterification

| Catalyst | Initial rate (mmol/mL-h) | Initial rate (mmol/g cat-h) | Initial TOF (h ⁻¹) |
|---------------------------------------|-----------------------------|--------------------------------|--------------------------------|
| CaO/Al ₂ O ₃ | 0.01 | 0.15 | 0.19 |
| Li-CaO/Al ₂ O ₃ | 0.004 | 0.06 | 0.04 |
| K-CaO/Al ₂ O ₃ | 0.14 | 2.01 | 0.84 |
| Sr-CaO/Al ₂ O ₃ | 0.03 | 0.47 | 0.20 |
| Fe-CaO/Al ₂ O ₃ | 0.02 | 0.30 | 0.19 |

4.2.4 Effect of leaching problem of CaO/Al₂O₃ pellet catalysts with different metal oxide on the catalytic activity of transesterification

The leaching of the catalyst is one of the important issues in biodiesel production, since prolonged leaching not only reduces the biodiesel yield and

product quality, but also causes product contamination. Furthermore, the leaching can reduce the reusability and sustainability of heterogeneous catalysts leading to the increment in price of catalyst replacement. Figure 4.11 presents the leaching results of different metal oxide loading on CaO/Al₂O₃ pellet catalysts. It was clear that the methanol solution obtained from K-CaO/Al₂O₃ pellet catalyst gave the highest biodiesel yield as 35%. This indicated that K⁺ ions and Ca²⁺ ions were dissolved in methanol solution to catalyze transesterification. In contrast, the biodiesel yield using the other catalysts were less than 1% of the resulting biodiesel yield. Since catalyst preparation by incipient wetness impregnation can promote interaction between Ca and metal oxide precursor (Ca-M) to anchor on surface of catalyst [64, 67] including metal oxide lowest dissolve in methanol or organic solution. According to the report of Mahmudah et al. [81], the Fe₂O₃-CaO catalyst can reduce leaching problem of Ca²⁺ and reused for 5 cycles. Similarly to the report by Zang et al. [71] who synthesized SrO-CaO-Al₂O₃ powder catalyst. Loading of SrO on Ca-Al catalyst can suppress the Ca²⁺ leaching problem. Kaur and Ali [82] studied the reusability of lithium Li-CaO catalyst for 4 consecutive cycles and found that smallest amount of Li⁺ ions was leached. The biodiesel yield derived from leaching was about 5%. Therefore, the amount of Li⁺ leaching can assume no significant homogeneous contribution concerned in catalytic activity which was corresponded to our study. However, some research found that the leaching problem was more remarkable when loading of Li⁺ species on the CaO catalyst to catalyze transesterification [83]. For the K⁺ ions leaching problem was in contrast to the report by Mabruro et al. [84]. They found that the potassium loaded on CaO/ZnO catalyst can be reused for 3 consecutive cycles to produce biodiesel without the leaching evidence. This might be due to the incorporated ZnO can reduce the K⁺ ions leaching to provide high efficiency of biodiesel production.

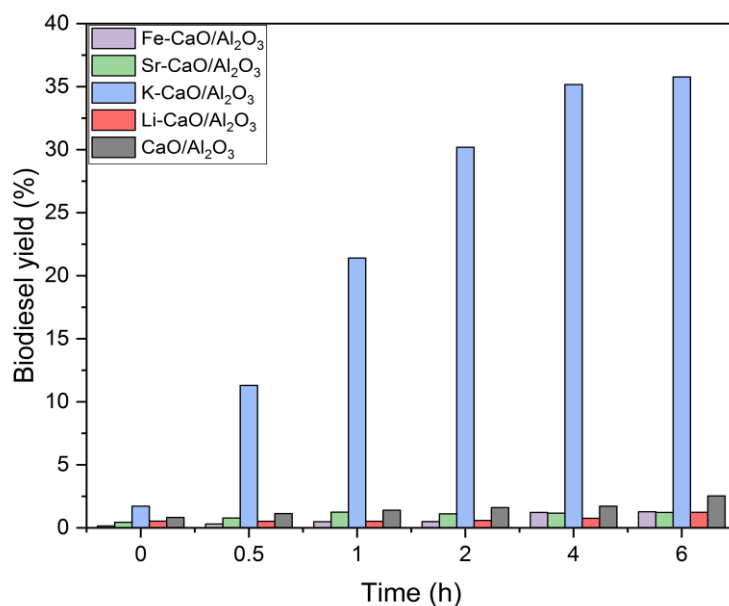


Figure 4.11 Effect of leaching problem on CaO/Al₂O₃ pellet catalysts with different metal oxide on the catalytic activity of transesterification

4.2.4 Comparison of catalytic activity in transesterification between other literature and in this study

Table 4.8 summarizes some catalytic performance reported literature of different catalysts in powder and extruded forms for transesterification. For comparison of their catalytic activities of transesterification with our study CaO/Al₂O₃ pellet catalysts using different metal oxides. This catalyst can be used under the mild conditions. Meanwhile, some literature provided the higher biodiesel yield. A few studies focused on the pellet or extruded catalyst to catalyze transesterification. Only two of researches works studied the catalyst forming to catalyze transesterification. Marinković et al. [9] demonstrated a good catalytic activity of CaO/Al₂O₃ spherical-pellet catalyst for biodiesel production under the following conditions: 60 °C, 5 h, 900 rpm, 12:1 methanol to oil molar ratio, and catalyst loading 0.5 wt.%. Although, the higher biodiesel yield of 94.3 %, was achieved, the leaching of calcium ions was observed which was 5 times greater than our pellet catalysts except K-CaO/Al₂O₃ pellet catalyst. Junior et al. [47] prepared 35 wt.% of K₂CO₃/Al₂O₃

hollow cylindrical catalyst with high surface area of 65 m²/g. A high temperature of reaction was carried out at 80 °C to obtain high biodiesel yield of 99% at 5 h. Furthermore, the higher methanol to oil molar ratio (18:1 and 20:1) using the powder catalyst to achieve a high biodiesel production as can be found from previous researches [48], [58], [71], [65] and [76]. Powder catalysts are notoriously difficult to separate from the reaction solution. Also, a crucial factor based on their particle size of powder catalysts, which are typically very small. It can produce unwanted agglomeration in the reactional media which reducing their catalytic performance. Therefore, the comparison of CaO/Al₂O₃ pellet catalysts using different metal oxides loading and CaO-based catalysts in terms of overall catalytic performance. This result found that a high biodiesel yield (>90%) was obtained under mild reaction conditions as a 65 °C reaction temperature, 600 rpm, 12:1 of methanol to palm oil ratio, 10 wt.% of catalyst loading and 6 h. Moreover, the mass transfer limitation and the leaching problem of heterogenous catalyst could be minimized by using metal oxides loading on CaO/Al₂O₃ pellet catalysts for biodiesel production.

Table 4.8 Summary of base catalysts for transesterification

| Catalyst | Catalyst shape | Calcination condition | Reaction conditions | | | | | Alcohol to oil | Biodiesel yield | Leaching of species | Ref. |
|--|--------------------|-----------------------|---------------------|------------------|----------|------------------------|------|----------------|---------------------------|---------------------|------|
| | | | Oil feedstock | Temperature (°C) | Time (h) | Catalyst weight (wt.%) | | | | | |
| CaO/Al ₂ O ₃ | Powder | 718 °C, 5 h | Palm oil | 65 | 5 | 6 | 12:1 | 98.64 | Ca ²⁺ | [85] | |
| CaO/Al ₂ O ₃ | Spherical | 475 °C, 4 h | Sunflower oil | 60 | 5 | 0.5 | 12:1 | 94.3 | Ca ²⁺ | [9] | |
| K ₂ CO ₃ /Al ₂ O ₃ | Hollow cylindrical | 500 °C, 4 h | Sunflower oil | 80 | 5 | 4 | 12:1 | 99.3 | - | [47] | |
| K ₂ O-CaO/ZnO | Powder | 600 °C, 3 h | Soybean oil | 60 | 6 | 4 | 15:1 | 81.08 | - | [51] | |
| Li-CaO | Powder | 850 °C, 4 h | Waste canola oil | 60 | 3 | 4 | 18:1 | 96.6 | - | [58] | |
| Li-CaO | Powder | 800 °C, 2 h | Nahor oil | 65 | 6 | 5 | 10:1 | 94 | - | [51] | |
| SrO-CaO-Al ₂ O ₃ | Powder | 850 °C, 4 h | Palm oil | 65 | 3 | 7.5 | 18:1 | 98.16 | Ca ²⁺ 0.31% | [71] | |
| CaO-SrO | Powder | 750 °C, 6 h | Cotton seed oil | 60 | 2 | 3.5 | 12:1 | 97.3 | - | [48] | |

Table 4.8 Summary of base catalysts for transesterification (Cont.)

| Catalyst | Catalyst shape | Calcination condition | Reaction conditions | | | | | Biodiesel yield | Leaching of species | Ref. |
|--------------------------------------|----------------|-----------------------|-------------------------|------------------|----------|------------------------|----------------|-----------------|---|---------------|
| | | | Oil feedstock | Temperature (°C) | Time (h) | Catalyst weight (wt.%) | Alcohol to oil | | | |
| Fe/Ca/Al ₂ O ₃ | Powder | 800 °C, 5 h | Refine used cooking oil | 65 | 3 | 6 | 18:1 | 81.31 | - | [65] |
| Ca/Fe | Powder | 600 °C, 5 h | Low grade unrefined oil | 120 | 1 | 6 | 20:1 | 99.5 | Ca ²⁺ and Fe ⁵⁺ | [76] |
| K-CaO/Al ₂ O ₃ | Cylindrical | 800 °C, 5 h | Palm oil | 65 | 6 | 10 | 12:1 | 95.5 | K ⁺ and Ca ²⁺ 35% | In this study |

CHAPTER 5

CONCLUSIONS

5.1 Conclusions

The CaO/Al₂O₃ pellet catalysts using aluminum as a binder, guar gum, silica sol and polyacrylamide as a pore forming agent were synthesized. The 20 wt.% of metal oxides loading on CaO/Al₂O₃ pellet catalysts were prepared by incipient wetness impregnation method using calcination temperature of 800 °C. The effect of size of CaO/Al₂O₃ pellet catalyst and different metal oxide type loading on CaO/Al₂O₃ pellet catalysts were investigated the catalytic activities for transesterification. The transesterification of palm oil was carried out in a batch reactor (75 mL round bottom 3-necks glass flask) with a stirring speed of 600 rpm, 12 to 1 of methanol to palm oil molar ratio, 10 wt.% of catalyst loading and a reaction temperature of 65°C for 6 h. The bare CaO/Al₂O₃ pellet catalyst and different metal oxide loading CaO/Al₂O₃ pellet catalysts were characterized by TGA, XRD, FT-IR, SEM/EDX CO₂-TPD, Hammett indicators and mechanical strength. In addition, leaching problem of CaO/Al₂O₃ pellet catalysts for catalytic activity were also investigated.

The K-CaO/Al₂O₃ pellet catalyst gave the highest biodiesel yield of 95.5 % under the similar reaction conditions while, the other metal oxide loading CaO/Al₂O₃ pellet catalysts provided the lower biodiesel yield. This result was corresponding to the total basicity from both CO₂-TPD, and Hammett indicators results. Basicity of the biodiesel catalyst is one of important factors affecting the catalyst activity in transesterification. Furthermore, the initial TOF of K-CaO/Al₂O₃ pellet catalyst was the highest value at 0.83 h⁻¹ which can reduce the induction period of reaction. The mechanical strength of the metal oxide loading on CaO/Al₂O₃ pellet catalysts was increased compared to bare CaO/Al₂O₃ pellet catalyst. Unfortunately, leaching problem of K-CaO/Al₂O₃ pellet catalyst was found that the high of K⁺ species ions were dissolved in methanol solution compared with other metal oxide loading on CaO/Al₂O₃ pellet catalyst. Therefore, it should be further investigated the method to avoid K⁺ species ions leaching from CaO/Al₂O₃ catalyst for the sustainability biodiesel production.

5.2 Recommendation

The following recommendations based on the experimental results

5.2.1 The single metal loading on $\text{CaO}/\text{Al}_2\text{O}_3$ pellet catalyst should be further investigated the catalytic activity in the packed bed reactor for commercial process.

5.2.2 Leaching problem of $\text{CaO}/\text{Al}_2\text{O}_3$ pellet catalyst could be further investigated using different co-metal species to improve catalytic activity for transesterification.

5.2.3 Using the co-metal oxide loading might improve the catalytic activity and stability of $\text{CaO}/\text{Al}_2\text{O}_3$ pellet catalyst for transesterification such as Li-Fe and Sr-Fe doped on $\text{CaO}/\text{Al}_2\text{O}_3$ pellet catalysts.





APPENDIX

จุฬาลงกรณ์มหาวิทยาลัย
CHULALONGKORN UNIVERSITY

APPENDIX A
CALCULATIONS

A.1 Mass of oil, methanol and catalyst

From density equation $\rho = \frac{\text{mass}}{\text{volume}} = \frac{m}{V}$ (A.1)

From moles equation $\text{mol} = \frac{\text{mass}}{\text{molecular weight}} = \frac{m}{MW}$ (A.2)

V of round bottom 3-neck glass flask = 150 mL ($V_{\text{total}} = \frac{3}{4}$ in 3-neck glass flask)

$V_{\text{oil}} = 50 \text{ mL}$

Where m of oil (ρ of oil = 0.89 g/mL, $V_{\text{oil}} = 50 \text{ mL}$)

$$\begin{aligned} m_{\text{oil}} &= \rho \times V_{\text{oil}} \\ m_{\text{oil}} &= (0.89 \text{ g/mL})(50 \text{ mL}) \\ m_{\text{oil}} &= 44.5 \text{ g} \end{aligned}$$

Where n of oil (MW of oil = 847 g/mol)

$$\begin{aligned} \text{mol}_{\text{oil}} &= \frac{m}{MW} \\ \text{mol}_{\text{oil}} &= \frac{44.5}{847} = 0.0525 \text{ mol} \end{aligned}$$

When the ratio of methanol to palm oil is 12 to 1

$$\begin{aligned} \text{mol}_{\text{MeOH}} &= \text{mol}_{\text{oil}} \times 12 \\ \text{mol}_{\text{MeOH}} &= (0.0525 \text{ mol})(12) = 0.63 \text{ mol} \end{aligned}$$

Where m of methanol (MW of methanol = 32.04 g/mol)

$$\begin{aligned} m_{\text{MeOH}} &= \text{mol}_{\text{MeOH}} \times MW \\ m_{\text{MeOH}} &= (0.63 \text{ mol})(32.04 \text{ g/mol}) = 20.19 \text{ g} \end{aligned}$$

Where V_{MeOH} (ρ of methanol 0.792 g/mL)

From $\rho = \frac{m}{V}$

$$\begin{aligned} V_{\text{MeOH}} &= \frac{m}{\rho} \\ V_{\text{MeOH}} &= \frac{20.19 \text{ g}}{0.792 \text{ g/mL}} = 25.49 \text{ mL} \end{aligned}$$

Example of calculating the weight of catalyst of the reaction oil using 10 % wt. of catalyst content.

When m of oil 44.5 g; catalyst weight = $(44.5 \text{ g}) \left(\frac{10}{100} \right) = 4.45 \text{ g}$

Where $V_{\text{total}} = V_{\text{oil}} + V_{\text{MeOH}}$; $V_{\text{total}} = 50 \text{ mL} + 16 \text{ mL} = 66 \text{ mL}$

A.2 Preparation of metal doping on CaO/Al₂O₃ pellet catalyst

Example K-CaO/Al₂O₃ pellet catalyst

From binder 2.5 g and CaO:binder = 3.5:1

$$\text{So, CaO} = 2.5 \times 3.5 = 8.75 \text{ g}$$

Molecular weight of CaCO₃ = 100.087 g/mol

Molecular weight of CaO = 56.077 g/mol

From 1 mole CaO = 1 mole CaCO₃

$$\text{Mole of CaO} = \frac{8.75 \text{ g}}{56.077 \text{ g/mol}} = 0.156 \text{ mol}$$

$$\text{So, using CaCO}_3 \text{ precursor} = 0.156 \text{ mol} \times 100.087 \text{ g/mol} = 15.57 \text{ g}$$

20 wt.% of K₂O metal doping

Using CaO/Al₂O₃ pellet catalyst is 4.45 g (10 wt.% catalyst based on oil)

From KNO₃ precursor

Molecular weight of K₂O = 94.196 g/mol

Molecular weight of KNO₃ = 101.032 g/mol

$$\text{Weight of K}_2\text{O} = \frac{4.45 \text{ g} \times 20}{100} = 0.89 \text{ g}$$

$$\text{Mole of K}_2\text{O} = \frac{0.89 \text{ g}}{94.196 \text{ g/mol}} = 0.009 \text{ mol}$$

$$\text{So, using KNO}_3 \text{ precursor} = \frac{0.89 \text{ g} \times 101.032 \text{ g/mol}}{94.196 \text{ g/mol}} = 0.860 \text{ g}$$

Metal oxide to calcium oxide mole ratio

$$\text{K}_2\text{O/CaO} = \frac{0.009}{0.156} = 0.061$$

Determine atomic ratio of K/Ca

Molecular weight of K = 39.1 g/mol

Molecular weight of Ca = 40.1 g/mol

$$\text{Weight of K} = \frac{0.89 \times 39.1}{94.196} = 0.369 \text{ g}$$

$$\text{Mole of K} = \frac{0.369}{39.1} = 0.01 \text{ mole}$$

$$\text{Weight of Ca in catalyst} = \frac{4.45 \times 40.1}{56.077} = 3.182 \text{ g}$$

$$\text{Mole of Ca in catalyst} = \frac{3.182 \text{ g}}{40.1 \text{ g/mol}} = 0.079 \text{ mole}$$

Metal to calcium mole ratio

$$K/\text{Ca} = \frac{0.01 \text{ mol}}{0.079 \text{ mol}} = 0.128$$

Table A.1 Metal oxide ratio and atomic ratio

| Catalyst | MO/CaO ratio | M/Ca ratio |
|---------------------------------------|--------------|------------|
| K-CaO/Al ₂ O ₃ | 0.061 | 0.128 |
| Li-CaO/Al ₂ O ₃ | 0.019 | 0.087 |
| Sr-CaO/Al ₂ O ₃ | 0.055 | 0.221 |
| Fe-CaO/Al ₂ O ₃ | 0.035 | 0.178 |

A.3 Crystallize size

The crystallite size of catalysts were determined by Debye Scherer equation as show in Eq (A.3)

$$d = \frac{K \lambda}{\beta_{FWHM} \cos \theta} \quad (\text{A.3})$$

Where d is crystallite size (\AA), K is the Scherrer constant which is 0.9 for spherical crystallites with cubic symmetry, λ is the X-ray wavelength (1.54 \AA), β_{FWHM} is the width (full-width at half-maximum) of the X-ray diffraction peak in radians and θ is the diffraction angle.

Example of crystallite size of CaO calculation was exhibited following Eq. (A.3).

The diffraction peak at $2\theta = 32.21614^\circ$ and $\beta_{FWHM} = 0.027568$ were selected to calculate. First, K and λ were substituted in Scherrer's equation.

From Eq. (A.3)

$$d = \frac{0.9 \times 1.54}{0.027568 \times \cos(16.10807)}$$

$$d = 51.77 \text{ \AA} = 5.177 \text{ nm}$$

Table A.2 Crystallize size of CaO

| 2θ | β_{FWHM} | d (nm) |
|-----------|----------------|--------|
| 32.21614 | 0.027568 | 5.177 |
| 32.27770 | 0.023114 | 6.175 |
| 32.46124 | 0.007871 | 18.142 |
| 32.28682 | 0.016345 | 8.733 |
| 32.21614 | 0.005472 | 26.080 |

A.4 Basicity of catalysts

The basicity of catalysts was measured by CO₂-TPD technique and determined total basicity of catalyst follow by equation A.4 from calibration curve in Figure A.1

$$Y = 29.481X \quad (\text{A.4})$$

Where y is the amount of adsorbed CO₂ in catalyst and x is total area of TCD signal.

Example of total basicity (mmol/g cat) of CaO/Al₂O₃ calculation was exhibited following Eq. (A.4). CO₂-TPD profile of CaO/Al₂O₃ was shown in Figure A.2.

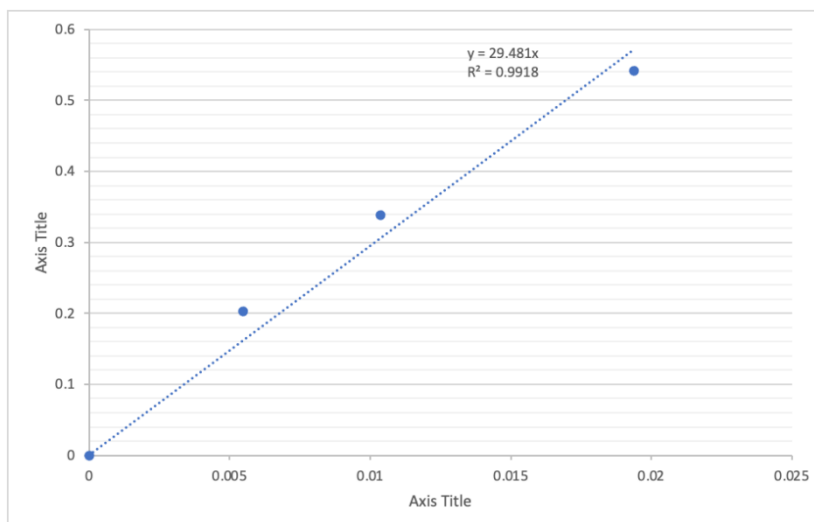


Figure A.1 Calibration curve of CO₂-TPD

From Eq. (A.4), total area of medium range = 0.191, strong range = 1.395 and 0.06 g of catalyst

At medium range

$$y = 29.481X$$

$$y = 29.481(0.191)$$

$$y = 5.623 \mu\text{mol} = 0.0056 \text{ mmol}$$

$$y = \frac{0.0056}{0.06} = 0.093 \text{ mmol/g}$$

At strong range

$$y = 29.481X$$

$$y = 29.481(1.395)$$

$$y = 41.122 \mu\text{mol} = 0.0411 \text{ mmol}$$

$$y = \frac{0.0411}{0.06} = 0.685 \text{ mmol/g}$$

Total basicity of $\text{CaO}/\text{Al}_2\text{O}_3 = 0.093 + 0.685 = 0.778 \text{ mmol/g cat}$

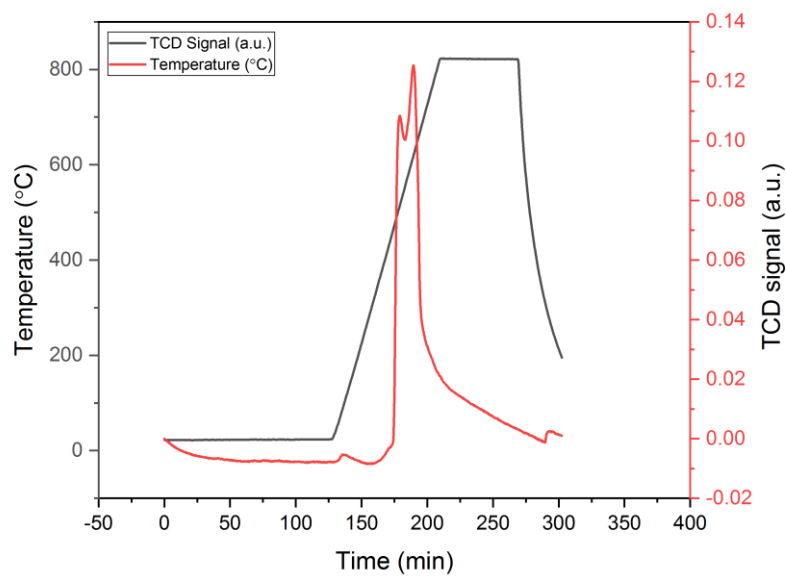


Figure A.2 CO_2 -TPD profile of $\text{CaO}/\text{Al}_2\text{O}_3$ pellet catalyst

Example for the deconvolution of CO_2 -TPD peak area of medium range (200-450 °C) using Fityk program was shown in Figure A.3

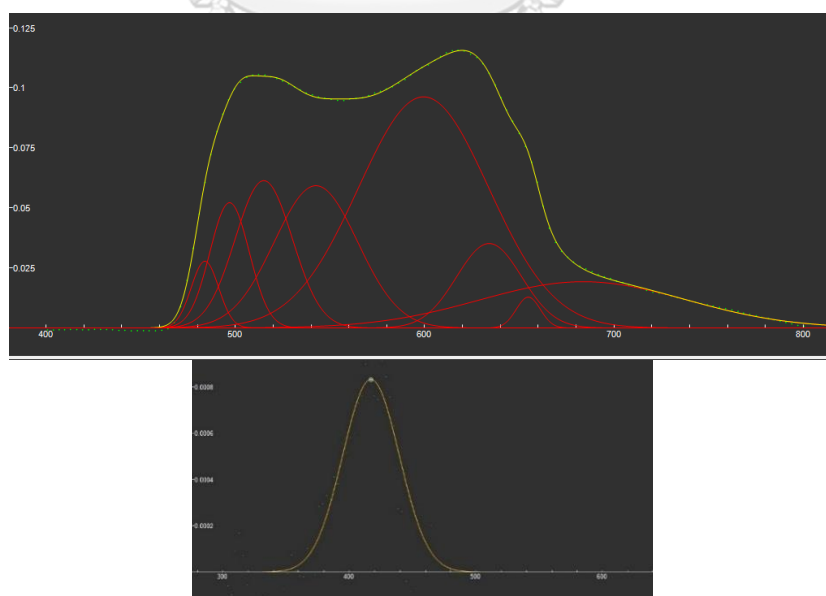


Figure A.3 Medium range peak from CO_2 -TPD technique

APPENDIX B

HAMMETT INDICATORS

B.1 Hammett indicators

To measure the basic strength and basicity of $\text{CaO}/\text{Al}_2\text{O}_3$ pellet catalyst using Hammett indicator method was performed as shown below.

Step 1 0.3 g of $\text{CaO}/\text{Al}_2\text{O}_3$ pellet catalyst was added into methanol 10 mL and left for 2 h to reach equilibrium.

Step 2 The chosen indicator was then dropped into the solution to determine its basic strength (Figure B.1). After the solution was filtered using filter paper. The basic strength ranges from 7.2 to 9.8. The solution was titrated with 0.1 M benzoic acid.

Step 3 determines the basicity concentration



Figure B.1 Hammett indicators test

Example for determination of basicity of CaO/Al₂O₃ pellet catalyst

Form Benzoic acid 0.1 M and solution CaO/Al₂O₃ and methanol at 10 mL

$$(C_{\text{benzoic}})(V_{\text{benzoic}}) = (C_{\text{CaO/Al}_2\text{O}_3})(V_{\text{CaO/Al}_2\text{O}_3})$$

Bromothymol blue

$$(0.1 \text{ M})(0.4 \text{ mL}) = (C_{\text{CaO}})(10 \text{ mL})$$

$$(C_{\text{CaO/Al}_2\text{O}_3}) = \frac{(0.1 \text{ M})(0.4 \text{ mL})}{(10 \text{ mL})} = 0.004 \text{ M}$$

$$\left(\frac{0.009 \text{ mol}}{1000 \text{ mL}} \times 10 \text{ mL} \right) \times 1000 = 0.13 \text{ mmol/g cat}$$

Phenolphthalein

$$(0.1 \text{ M})(0.4 \text{ mL}) = (C_{\text{CaO}})(10 \text{ mL})$$

$$(C_{\text{CaO/Al}_2\text{O}_3}) = \frac{(0.1 \text{ M})(0.4 \text{ mL})}{(10 \text{ mL})} = 0.004 \text{ M}$$

$$\left(\frac{0.009 \text{ mol}}{1000 \text{ mL}} \times 10 \text{ mL} \right) \times 1000 = 0.13 \text{ mmol/g cat}$$

So, total basicity of CaO/Al₂O₃ pellet catalyst = 0.13 + 0.13 = 0.26 mmol/g cat

APPENDIX C

Biodiesel YIELD

C.1 Biodiesel yield

The biodiesel yield was analyzed by gas chromatograph (GC) and determine biodiesel yield by Eq. (A.5)

$$\text{FAME yield (\%)} = \frac{\sum A_{\text{FAME}}}{A_{\text{Ref}}} \times \frac{m_{\text{Ref}}}{m_{\text{FAME}}} \times 100\% \quad (\text{A.5})$$

Where A_{FAME} , A_{Ref} , m_{Ref} and m_{FAME} refer to the area of FAME, area of biodiesel standard, mass of FAME (g) and mass of biodiesel standard (g), respectively obtained by gas chromatography analysis

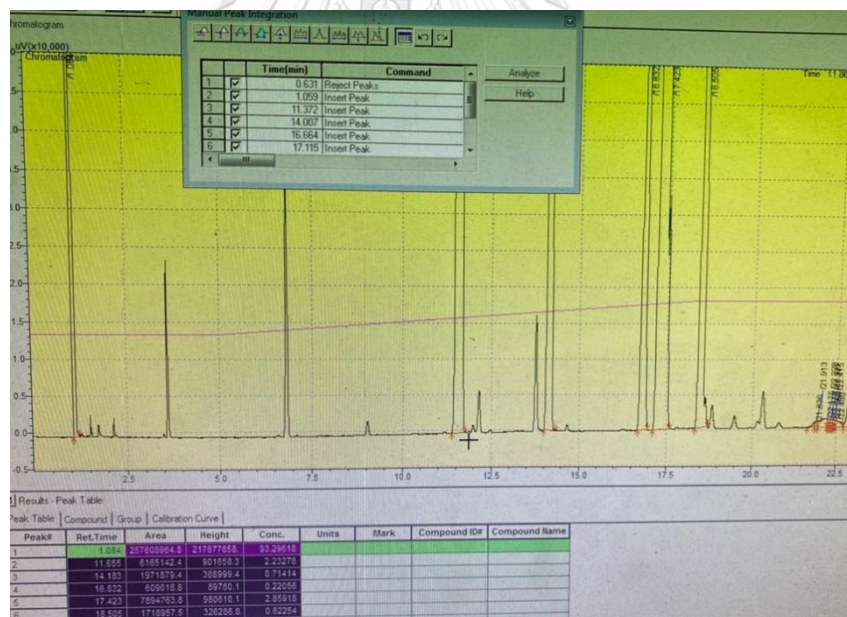


Figure C.1 The biodiesel yield was analyzed by gas chromatograph (GC)

APPENDIX D

THE INITIAL TOF

D.1 The initial TOF

The initial TOF was determined by initial rate and total basicity by CO₂-TPD measurement, following by Eq. (A.6).

$$\text{The initial TOF (time}^{-1}\text{)} = \frac{\text{Initial rate of oil consumption}}{\text{total basicity of catalyst}} \quad (\text{A.6})$$

Where the initial rate of oil consumption is in mmol/mL-g cat and total basicity is in mmol/g cat.

Example for determination of initial rate of transesterification reaction under condition 12 to 1 of methanol to palm oil ratio, 10 wt.% of catalyst loading and a reaction temperature of 65°C after 1 h. of CaO/Al₂O₃ was shown in Figure D.1

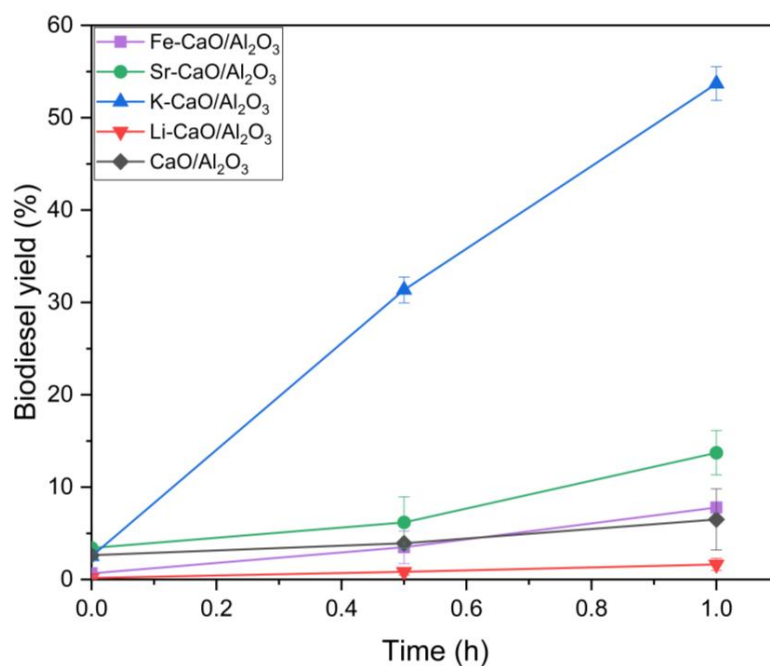


Figure D.1 Biodiesel yield after 1 h of metal oxides loading on CaO/Al₂O₃ pellet catalyst

Assumed oil is the limiting reaction

Mol oil = 0.0525 mol

Catalyst weight loading = 4.45 g

Reaction volume = 66 mL

Catalyst in reaction = 0.067 g/mL

Basicity of CaO/Al₂O₃ pellet catalyst by CO₂-TPD technique = 0.78 mmol/g cat

To calculation initial rate by slope of reaction (Biodiesel yield VS. reaction time)

From Slope = $\frac{\Delta y}{\Delta x}$, at t=0, y=0.0264 and at t=1, y= 0.0650

$$\text{Slope} = \frac{0.0650 - 0.0264}{1 - 0} = 0.039 \text{ h}^{-1}$$

From initial rate = $\frac{0.039 \times 0.0525 \text{ mol}}{66 \text{ mL} \times 3} = 0.0000103 \text{ mol/mL-h} = 0.01 \text{ mmol/mL-h}$

$$\text{initial rate} = \frac{0.01 \frac{\text{mmol}}{\text{mL-h}}}{0.067 \text{ g cat/mL}} = 0.15 \text{ mmol/g cat-h}$$

So, initial TOF (time⁻¹) = $\frac{0.15 \frac{\text{mmol}}{\text{g cat-h}}}{0.78 \frac{\text{mmol}}{\text{g cat}}} = 0.19 \text{ h}^{-1}$

REFERENCES

- [1] E.-F.R. Energies, Transesterification in biodiesel, 2004.
- [2] G. Chen, R. Shan, J. Shi, C. Liu, B. Yan, Biodiesel production from palm oil using active and stable K doped hydroxyapatite catalysts, *Energy Conversion and Management*, 98 (2015) 463-469.
- [3] J. Marchetti, V. Miguel, A. Errazu, Possible methods for biodiesel production, *Renewable and Sustainable Energy Reviews*, 11 (2007) 1300-1311.
- [4] M. Khatibi, F. Khorasheh, A. Larimi, Biodiesel production via transesterification of canola oil in the presence of Na-K doped CaO derived from calcined eggshell, *Renewable Energy*, 163 (2021) 1626-1636.
- [5] P.T. Vasudevan, M. Briggs, Biodiesel production—current state of the art and challenges, *Journal of Industrial Microbiology and Biotechnology*, 35 (2008) 421.
- [6] P. Mierczynski, K.A. Chalupka, W. Maniukiewicz, J. Kubicki, M.I. Szykowska, T.P. Maniecki, SrAl₂O₄ spinel phase as active phase of transesterification of rapeseed oil, *Applied Catalysis B: Environmental*, 164 (2015) 176-183.
- [7] J. Gupta, M. Agarwal, A. Dalai, An overview on the recent advancements of sustainable heterogeneous catalysts and prominent continuous reactor for biodiesel production, *Journal of Industrial and Engineering Chemistry*, (2020).
- [8] Y. Tang, J. Xu, J. Zhang, Y. Lu, Biodiesel production from vegetable oil by using modified CaO as solid basic catalysts, *Journal of Cleaner Production*, 42 (2013) 198-203.
- [9] D.M. Marinković, J.M. Avramović, M.V. Stanković, O.S. Stamenković, D.M. Jovanović, V.B. Veljković, Synthesis and characterization of spherically-shaped CaO/γ-Al₂O₃ catalyst and its application in biodiesel production, *Energy Conversion and Management*, 144 (2017) 399-413.
- [10] E.G.S. Junior, O.R. Justo, V.H. Perez, F. da Silva Melo, I. Reyero, A. Serrano-Lotina, F.J. Mompean, Biodiesel synthesis using a novel monolithic catalyst with magnetic properties (K₂CO₃/γ-Al₂O₃/Sepiolite/γ-Fe₂O₃) by ethanolic route, *Fuel*, 271 (2020) 117650.
- [11] A. Ravi, B. Gurunathan, N. Rajendiran, S. Varjani, E. Gnansounou, A. Pandey, S. You,

- J.K. Raman, P. Ramanujam, Contemporary approaches towards augmentation of distinctive heterogeneous catalyst for sustainable biodiesel production, *Environmental Technology & Innovation*, 19 (2020) 100906.
- [12] D.Y. Leung, X. Wu, M. Leung, A review on biodiesel production using catalyzed transesterification, *Applied energy*, 87 (2010) 1083-1095.
- [13] H. Li, F. Liu, Y. Helian, G. Yang, Z. Wu, Y. Gao, M. Guo, P. Cui, D. Wang, M. Yu, Inspection of various precipitant on SrO-based catalyst for transesterification: Catalytic performance, reusability and characterizations, *Catalysis Today*, 376 (2020) 197-204.
- [14] B. Tabah, A.P. Nagvenkar, N. Perkas, A. Gedanken, Solar-heated sustainable biodiesel production from waste cooking oil using a sonochemically deposited SrO catalyst on microporous activated carbon, *Energy & Fuels*, 31 (2017) 6228-6239.
- [15] S. Niu, X. Zhang, Y. Ning, Y. Zhang, T. Qu, X. Hu, Z. Gong, C. Lu, Dolomite incorporated with cerium to enhance the stability in catalyzing transesterification for biodiesel production, *Renewable Energy*, 154 (2020) 107-116.
- [16] A. P Singh Chouhan, A. K Sarma, Critical analysis of process parameters for bio-oil production via pyrolysis of biomass: A review, *Recent Patents on Engineering*, 7 (2013) 98-114.
- [17] S. Silsakulsook, Controlling quality of biodiesel, (2007); Available February 3, 2021 from <https://www.eria.org/Current%20Status%20of%20Biodiesel%20Fuel%20in%20East%20Asia%20and%20ASEAN%20Countries.pdf>.
- [18] D.o.E.B.M.o. Energy, Biodiesel standard. (2012); Available February 3, 2021 from <https://www.doeb.go.th/kmv2/report/biodiesel1.pdf>.
- [19] M. Balat, Production of biodiesel from vegetable oils: A survey, *Energy Sources, Part A*, 29 (2007) 895-913.
- [20] T.i.o.s.a.t. research, Production and biodiesel standard test. Available February 3, 2021 from http://www.ksp108.com/private_folder/bio200712.pdf.
- [21] C. company, Biodiesel and U.S diesel vehicle market. (2016); Available February 3, 2021 from <https://futurefuelcorporation.com/biodiesel-u-s-diesel-vehicle-market-2016/>.

- [22] P. Jenvanitpanjakul, Establishment of the Guidelines for the Development of Biodiesel Standards in the APEC Region, APEC 21st Century Renewable Energy Development Initiative (Collaborative IX), 2009, pp. 37.
- [23] R.F. IM, H. Ong, T. Mahlia, M. Mofijur, A. Silitonga, A.R. SM, A. Ahmad, State of the art of catalysts for biodiesel production, *Frontiers in Energy Research*, 8 (2020) 1-16.
- [24] Y.H. Tan, M.O. Abdullah, J. Kasedo, N.M. Mubarak, Y. San Chan, C. Nolasco-Hipolito, Biodiesel production from used cooking oil using green solid catalyst derived from calcined fusion waste chicken and fish bones, *Renewable Energy*, 139 (2019) 696-706.
- [25] A.S. Chouhan, A. Sarma, Modern heterogeneous catalysts for biodiesel production: A comprehensive review, *Renewable and Sustainable Energy Reviews*, 15 (2011) 4378-4399.
- [26] N.S. Talha, S. Sulaiman, Overview of catalysts in biodiesel production, *ARPN Journal of Engineering and Applied Sciences*, 11 (2016) 439-448.
- [27] M.K. Lam, K.T. Lee, A.R. Mohamed, Homogeneous, heterogeneous and enzymatic catalysis for transesterification of high free fatty acid oil (waste cooking oil) to biodiesel: A review, *Biotechnology Advances*, 28 (2010) 500-518.
- [28] E. Andrijanto, E. Dawson, D. Brown, Hypercrosslinked polystyrene sulphonic acid catalysts for the esterification of free fatty acids in biodiesel synthesis, *Applied Catalysis B: Environmental*, 115 (2012) 261-268.
- [29] A.F. Lee, J.A. Bennett, J.C. Manayil, K. Wilson, Heterogeneous catalysis for sustainable biodiesel production via esterification and transesterification, *Chemical Society Reviews*, 43 (2014) 7887-7916.
- [30] I. Atadashi, M. Aroua, A.A. Aziz, N. Sulaiman, The effects of catalysts in biodiesel production: A review, *Journal of Industrial and Engineering Chemistry*, 19 (2013) 14-26.
- [31] E. Lotero, Y. Liu, D.E. Lopez, K. Suwannakarn, D.A. Bruce, J.G. Goodwin, Synthesis of biodiesel via acid catalysis, *Industrial and Engineering Chemistry Research*, 44 (2005) 5353-5363.
- [32] K. Sudsakorn, S. Saiwuttikul, S. Palitsakun, A. Seubsai, J. Limtrakul, Biodiesel production from *Jatropha Curcas* oil using strontium-doped CaO/MgO catalyst, *Journal of Environmental Chemical Engineering*, 5 (2017) 2845-2852.

- [33] A.L. de Lima, C.M. Ronconi, C.J. Mota, Heterogeneous basic catalysts for biodiesel production, *Catalysis Science & Technology*, 6 (2016) 2877-2891.
- [34] M. Kouzu, J.-s. Hidaka, Transesterification of vegetable oil into biodiesel catalyzed by CaO: A review, *Fuel*, 93 (2012) 1-12.
- [35] I.B. Banković-Ilić, M.R. Miladinović, O.S. Stamenković, V.B. Veljković, Application of nano CaO-based catalysts in biodiesel synthesis, *Renewable and Sustainable Energy Reviews*, 72 (2017) 746-760.
- [36] D.M. Marinković, M.V. Stanković, A.V. Veličković, J.M. Avramović, M.R. Miladinović, O.O. Stamenković, V.B. Veljković, D.M. Jovanović, Calcium oxide as a promising heterogeneous catalyst for biodiesel production: Current state and perspectives, *Renewable and Sustainable Energy Reviews*, 56 (2016) 1387-1408.
- [37] A.A. Kiss, A.C. Dimian, G. Rothenberg, Solid acid catalysts for biodiesel production—towards sustainable energy, *Advanced Synthesis & Catalysis*, 348 (2006) 75-81.
- [38] F. Chang, Q. Zhou, H. Pan, X.F. Liu, H. Zhang, W. Xue, S. Yang, Solid mixed-metal-oxide catalysts for biodiesel production: A review, *Energy Technology*, 2 (2014) 865-873.
- [39] D.-W. Lee, Y.-M. Park, K.-Y. Lee, Heterogeneous base catalysts for transesterification in biodiesel synthesis, *Catalysis Surveys from Asia*, 13 (2009) 63-77.
- [40] H.H. Mardhiah, H.C. Ong, H. Masjuki, S. Lim, H. Lee, A review on latest developments and future prospects of heterogeneous catalyst in biodiesel production from non-edible oils, *Renewable and Sustainable Energy Reviews*, 67 (2017) 1225-1236.
- [41] B. Ali, S. Yusup, A.T. Quitain, M.S. Alnarabiji, R.N.M. Kamil, T. Kida, Synthesis of novel graphene oxide/bentonite bi-functional heterogeneous catalyst for one-pot esterification and transesterification reactions, *Energy Conversion and Management*, 171 (2018) 1801-1812.
- [42] B. Kraushaar-Czarnetzki, S.P. Muller, *Shaping of solid catalysts, synthesis of solid catalysts*, Wiley-VCH, Betz-druck GmbH, Darmstadt (2009). pp. 173-182.
- [43] N.V.K. S. DEVYATKOV¹, D.YU. MURZIN², On comprehensive understanding of catalyst shaping by extrusion, *Chemistry Today*, 19 (2015), pp. 57-64.
- [44] R. Klaewkla, M. Arend, W.F. Hoelderich, A review of mass transfer controlling the reaction rate in heterogeneous catalytic systems, INTECH Open Access Publisher

London 2011. pp. 1-19.

[45] E.G. Silveira Junior, O.R. Justo, V.H. Perez, I. Reyero, A. Serrano-Lotina, L. Campos Ramirez, D.F. dos Santos Dias, Extruded catalysts with magnetic properties for biodiesel production, *Advances in Materials Science and Engineering*, 2018 (2018) 1-12.

[46] P. Lu, H. Wang, K. Hu, Synthesis of glycerol carbonate from glycerol and dimethyl carbonate over the extruded CaO-based catalyst, *Chemical Engineering Journal*, 228 (2013) 147-154.

[47] E.G.S. Junior, V.H. Perez, I. Reyero, A. Serrano-Lotina, O.R. Justo, Biodiesel production from heterogeneous catalysts based K_2CO_3 supported on extruded $\gamma-Al_2O_3$, *Fuel*, 241 (2019) 311-318.

[48] G. Anastopoulos, G. Dodos, S. Kalligeros, F. Zannikos, CaO loaded with $Sr(NO_3)_2$ as a heterogeneous catalyst for biodiesel production from cottonseed oil and waste frying oil, *Biomass Conversion and Biorefinery*, 3 (2013) 169-177.

[49] S. Palitsakun, K. Koonkuer, B. Topool, A. Seubsai, K. Sudsakorn, Transesterification of Jatropha oil to biodiesel using SrO catalysts modified with CaO from waste eggshell, *Catalysis Communications*, 149 (2021) 106233.

[50] A. Al-Saadi, B. Mathan, Y. He, Esterification and transesterification over SrO–ZnO/ Al_2O_3 as a novel bifunctional catalyst for biodiesel production, *Renewable Energy*, 158 (2020) 388-399.

[51] J. Boro, L.J. Konwar, D. Deka, Transesterification of non edible feedstock with lithium incorporated egg shell derived CaO for biodiesel production, *Fuel Processing Technology*, 122 (2014) 72-78.

[52] Y. Liu, P. Zhang, M. Fan, P. Jiang, Biodiesel production from soybean oil catalyzed by magnetic nanoparticle $MgFe_2O_4@CaO$, *Fuel*, 164 (2016) 314-321.

[53] M. Yahaya, I. Ramli, E.N. Muhamad, N.S. Ishak, U. Idris Nda-Umar, Y.H. Taufiq-Yap, K_2O Doped Dolomite as Heterogeneous Catalyst for Fatty Acid Methyl Ester Production from Palm Oil, *Catalysts*, 10 (2020) 791.

[54] N.F. Sulaiman, S.L. Lee, S. Toemen, W.A.W.A. Bakar, Physicochemical characteristics of Cu/Zn/ $\gamma-Al_2O_3$ catalyst and its mechanistic study in transesterification for biodiesel production, *Renewable Energy*, 156 (2020) 142-157.

- [55] J. Jitjamnong, A. Luengnaruemitchai, N. Samanwonga, N. Chuaykarn, Biodiesel production from canola oil and methanol using Ba impregnated calcium oxide with microwave irradiation-assistance, *Chiang Mai Journal Science*, 46 (2019) 987-1000.
- [56] E.S. Umdu, E. Seker, Transesterification of sunflower oil on single step sol-gel made Al_2O_3 supported CaO catalysts: Effect of basic strength and basicity on turnover frequency, *Bioresource Technology*, 106 (2012) 178-181.
- [57] J. Zheng, G. Tan, P. Shan, T. Liu, J. Hu, Y. Feng, L. Yang, M. Zhang, Z. Chen, Y. Lin, Understanding thermodynamic and kinetic contributions in expanding the stability window of aqueous electrolytes, *Chem Catalysis*, 4 (2018) 2872-2882.
- [58] M. AlSharifi, H. Znad, Development of a lithium based chicken bone (Li-Cb) composite as an efficient catalyst for biodiesel production, *Renewable Energy*, 136 (2019) 856-864.
- [59] K. Hu, H. Wang, Y. Liu, C. Yang, KNO_3/CaO as cost-effective heterogeneous catalyst for the synthesis of glycerol carbonate from glycerol and dimethyl carbonate, *Journal of Industrial and Engineering Chemistry*, 28 (2015) 334-343.
- [60] C. Sun, Y. Guo, X. Xu, Q. Du, H. Duan, Y. Chen, H. Li, H. Liu, In situ preparation of carbon/ Fe_3C composite nanofibers with excellent electromagnetic wave absorption properties, *Composites Part A: Applied Science and Manufacturing*, 92 (2017) 33-41.
- [61] M.L. Ruiz, I.D. Lick, M.I. Ponzi, E.R. Castellón, A. Jiménez-López, E.N. Ponzi, Thermal decomposition of supported lithium nitrate catalysts, *Thermochimica Acta*, 499 (2010) 21-26.
- [62] M. Sulaiman, A. Rahman, N. Mohamed, Effect of water-based sol gel method on structural, thermal and conductivity properties of $\text{LiNO}_3\text{-Al}_2\text{O}_3$ composite solid electrolytes, *Arabian Journal of Chemistry*, 10 (2017) 1147-1152.
- [63] H. Husin, T. Asnawi, A. Firdaus, H. Husaini, I. Ibrahim, F. Hasfita, Solid catalyst nanoparticles derived from oil-palm empty fruit bunches (Op-Efb) as a renewable catalyst for biodiesel production, *IOP Conference Series: Materials Science and Engineering*, IOP Publishing, 2018, pp. 012008.
- [64] H. Li, S. Niu, C. Lu, J. Li, Calcium oxide functionalized with strontium as heterogeneous transesterification catalyst for biodiesel production, *Fuel*, 176 (2016) 63-71.

- [65] N.F. Sulaiman, A.N.N. Hashim, S. Toemen, S.J.M. Rosid, W.N.A.W. Mokhtar, R. Nadarajan, W.A.W.A. Bakar, Biodiesel production from refined used cooking oil using co-metal oxide catalyzed transesterification, *Renewable Energy*, 153 (2020) 1-11.
- [66] D.M. Alonso, R. Mariscal, M.L. Granados, P. Maireles-Torres, Biodiesel preparation using Li/CaO catalysts: activation process and homogeneous contribution, *Catalysis Today*, 143 (2009) 167-171.
- [67] D. Kumar, A. Ali, Nanocrystalline lithium ion impregnated calcium oxide as heterogeneous catalyst for transesterification of high moisture containing cotton seed oil, *Energy & fuels*, 24 (2010) 2091-2097.
- [68] T. Zhang, N. Zhao, J. Li, H. Gong, T. An, F. Zhao, H. Ma, Thermal behavior of nitrocellulose-based superthermites: Effects of nano-Fe₂O₃ with three morphologies, *Royal Society of Chemistry Advances*, 7 (2017) 23583-23590.
- [69] DOSEM, Detector warm up ,EDS Warm up,EDX Warm up, Website, 2013.
- [70] M. Thommes, K. Kaneko, A.V. Neimark, J.P. Olivier, F. Rodriguez-Reinoso, J. Rouquerol, K.S. Sing, Physisorption of gases, with special reference to the evaluation of surface area and pore size distribution (IUPAC Technical Report), *Pure and Applied Chemistry*, 87 (2015) 1051-1069.
- [71] Y. Zhang, S. Niu, K. Han, Y. Li, C. Lu, Synthesis of the SrO–CaO–Al₂O₃ trimetallic oxide catalyst for transesterification to produce biodiesel, *Renewable Energy*, 168 (2021) 981-990.
- [72] L.C. Meher, M.G. Kulkarni, A.K. Dalai, S.N. Naik, Transesterification of karanja (*Pongamia pinnata*) oil by solid basic catalysts, *European Journal of Lipid Science and Technology*, 108 (2006) 389-397.
- [73] F. Jamil, P.S.M. Kumar, L. Al-Haj, M.T.Z. Myint, H. Ala'a, Heterogeneous carbon-based catalyst modified by alkaline earth metal oxides for biodiesel production: Parametric and kinetic study, *Energy Conversion and Management: X*, 10 (2021) 100047.
- [74] Y. Zhang, S. Niu, K. Han, Y. Li, C. Lu, Synthesis of the SrO–CaO–Al₂O₃ trimetallic oxide catalyst for transesterification to produce biodiesel, *Renewable Energy*, 168 (2020) 981-990.
- [75] Y. Jie, Y. Dinghua, S. Peng, H. HUANG, Alkaline earth metal modified NaY for lactic acid dehydration to acrylic acid: effect of basic sites on the catalytic performance,

Chinese Journal of Catalysis, 32 (2011) 405-411.

[76] T.-L. Kwong, K.-F. Yung, Heterogeneous alkaline earth metal–transition metal bimetallic catalysts for synthesis of biodiesel from low grade unrefined feedstock, Royal Society of Chemistry Advances, 5 (2015) 83748-83756.

[77] M. Shi, P. Zhang, M. Fan, P. Jiang, Y. Dong, Influence of crystal of Fe_2O_3 in magnetism and activity of nanoparticle $\text{CaO}@ \text{Fe}_2\text{O}_3$ for biodiesel production, Fuel, 197 (2017) 343-347.

[78] J.H.J. Ashutosh Namdeo, S. M. Mahajani, A. K. Suresh, Effect of mass transfer limitation on catalytic activity and selectivity for oxidation of glycerol, The 25th International Symposium on Chemical Reaction Engineering, Florence, Italy, 2018.

[79] T. Witoon, S. Bumrungsalee, P. Vathavanichkul, S. Palitsakun, M. Saisriyoot, K. Faungnawakij, Biodiesel production from transesterification of palm oil with methanol over CaO supported on bimodal meso-macroporous silica catalyst, Bioresource Technology, 156 (2014) 329-334.

[80] D. Kumar, A. Ali, Nanocrystalline K–CaO for the transesterification of a variety of feedstocks: Structure, kinetics and catalytic properties, Biomass and Bioenergy, 46 (2012) 459-468.

[81] S. Ezzah-Mahmudah, I.M. Lokman, M.I. Saiman, Y.H. Taufiq-Yap, Synthesis and characterization of $\text{Fe}_2\text{O}_3/\text{CaO}$ derived from Anadara Granosa for methyl ester production, Energy Conversion and Management, 126 (2016) 124-131.

[82] M. Kaur, A. Ali, Ethanolysis of waste cottonseed oil over lithium impregnated calcium oxide: Kinetics and reusability studies, Renewable Energy, 63 (2014) 272-279.

[83] J.F. Puna, J.F. Gomes, J.C. Bordado, M.J.N. Correia, A.P.S. Dias, Biodiesel production over lithium modified lime catalysts: Activity and deactivation, Applied Catalysis A: General, 470 (2014) 451-457.

[84] I. Istadi, U. Mabruro, B.A. Kalimantanini, L. Buchori, D.D. Anggoro, Reusability and stability tests of calcium oxide based catalyst ($\text{K}_2\text{O}/\text{CaO}-\text{ZnO}$) for transesterification of soybean oil to biodiesel, Bulletin of Chemical Reaction Engineering and Catalysis, 11 (2016) 34-39.

[85] M. Zabeti, W.M.A.W. Daud, M.K. Aroua, Biodiesel production using alumina-supported calcium oxide: An optimization study, Fuel processing technology, 91 (2010)

243-248.





จุฬาลงกรณ์มหาวิทยาลัย
CHULALONGKORN UNIVERSITY

VITA

NAME Nattawadee Munbupphachart

DATE OF BIRTH 03 July 1996

PLACE OF BIRTH Rayong

INSTITUTIONS ATTENDED Chemical Engineering, King Mongkut's University of Technology Thonburi, Bangkok, Thailand.

HOME ADDRESS 186/88, Saruta View village, Rimnam Rd, Choeng Noen, Muang, Rayong 21000.

